Supplement of Aerosol Research, 3, 569–587, 2025 https://doi.org/10.5194/ar-3-569-2025-supplement © Author(s) 2025. CC BY 4.0 License.





Supplement of

Differentiating between Euro 5 gasoline and diesel light-duty engine primary and secondary particle emissions using multivariate statistical analysis of high-resolution mass spectrometry (HRMS) fingerprints

Camille Noblet et al.

Correspondence to: Francois Lestremau (francois.lestremau@mines-ales.fr) and Alexandre Albinet (alexandre.albinet@ineris.fr)

The copyright of individual parts of the supplement might differ from the article licence.

1 Vehicles tested, driving cycles and fuels

Table S1. Characteristics of the two tested vehicles.

Vehicle	N°1	N°2	
Type	1.4 TSI, 16V DSG7, ID	1.6 HDI ^c	
Fuel	Gasoline	Diesel	
Standard	Euro 5	Euro 5	
Empty weight (kg)	1285	1080	
Mileage (km)	92550	105823	
Gearbox (number of gears)	Sequential (7)	Manual (5)	
Post treatment system	TWC^a	DOC + Additive DPF ^b	
In-service date	10/21/2009	10/30/2013	

^aTWC: Three-way catalysis

^bDOC + Additive DPF: Diesel Oxidation Catalyst + Additive Diesel Particulate Filter

^cHDI: High pressure direct injection

Table S2. Main characteristics of the fuel used for the tested vehicles.

	Diesel B7	Gasoline SP95-E10
Colour	yellow	
Density at 15 °C (kg m ⁻³)	833.4	739.4
Sulphur content (mg kg ⁻¹)	9.7	8.7
Water content (mg kg ⁻¹)	100	
Total contamination (mg kg ⁻¹)	< 12	
Total aromatic hydrocarbons (% m)	27.8	
Polycyclic aromatic hydrocarbons (% m)	4.7	
Lead content (mg L ⁻¹)		< 2.5
Manganese content (mg L ⁻¹)		< 5.0
Benzene content (% m)		0.61
Ethanol content (% vol)		7.3
ETBE content (% vol)		5.74
Total oxygenated compounds (% vol)		13.29
Oxygen content (% m)		3.7
Aromatic content (% vol)		22.2
Olefin content (% vol)		15.3
Saturated content (% vol)		49.3

2 Sampling setup

Table S3. Overview of instruments used to measure the gas- and particulate-phase pollutants for the experiments.

Measured parameters	Phase	Sampling location	Instrument	Note
O_2	Gas	Emission and after dilution	Multigas analyzer PG250 (Horiba) Range: 0–25% in volume	Online
CO	Gas	Emission and after dilution	Multigas analyzer PG250 (Horiba) Range: 0–1000 ppm	Online
NO/NO _x	Gas	Emission	Multigas analyzer PG250 (Horiba) Range: 0–100 ppm	Online
INO/INO _X	Gas	After dilution	Model 42i (NO-NO ₂ -NO _x) Analyzer (Thermo) Range: 0–100 ppm	
CO_2	Gas	Emission	VA 3000 (Horiba) Range: 0–10000 ppm	Online
CO_2	Gas	After dilution	VA 3000 (Horiba) Range: 0–5000 ppm	
SO_2	Gas	After dilution	AF 21 M Environnement S.A. Range: 0–0.05 ppm	Online
O_3	Gas	After dilution	Model 202, 2B Technologies Range: 0–250 ppm	Online
Particle number	Particle	After dilution	CPC Grimm Serie 5.400 Range: 5-1000 nm CPC TSI 3775 Range: 4–1000 nm	Online
Non-refractory PM chemical composition	Particle	After dilution	Time of Flight-Aerosol Chemical Speciation Monitor (ToF-ACSM) Aerodyne Research Range: 40–1000 nm	Online

3 Non-target screening analyses

Table S4. List of solvents and chemicals used (suppliers and purity).

Compound	Supplier	Purity (%)			
Extraction and inje	Extraction and injection internal standards				
Beflubutamid-d ₇	HPC Standards	99.8			
Metsulfuron-d ₃	HPC Standards	99.6			
Succinic acid-d4	CDN Isotopes	99.0			
Nonanedioic acid-d ₁₄	CDN Isotopes	99.0			
¹³ C-Sulfamethazine	Sigma Aldrich	99.9			
Simazine-d ₁₀	Dr Ehrenstorfer	98.1			
Diuron-d ₆	Dr Ehrenstorfer	99.6			
¹³ C-Diclofenac	Dr Ehrenstorfer	97.7			
9,10-Anthraquinone-d ₈	CDN Isotopes	99.0			
1-Nitronaphthalene-d ₇	CDN Isotopes	98.3			
Benzo[g,h,i]perylene-d ₁₂	CDN Isotopes	99.4			
Pentadecane-d ₃₂	Sigma Aldrich	98.0			
Pentacosane-d ₅₂	CDN Isotopes	98.6			
Naphthalène-d ₈	Supelco	99.9			
2,2',5,5'-tetrachlorobiphenyl ¹³ C ₁₂ (PCB52*)	Wellington	98.0			
Perylene-d ₁₂	Cambridge Isotope Laboratories	99.0			
S	olvents				
Acetonitrile	Honeywell, Merck	99.9			
Methanol	Honeywell, Merck	99.9			
Acetic acid	Fischer Chemical	LC/MS Grade			
Ammonium acetate	Fischer Chemical	LC/MS Grade			
Water	Millipore	Milli-Q (18 M Ω)			

Table S5. Internal standard solutions with concentrations of compounds (µg mL⁻¹), mass, and retention time.

Internal standard	Concentration (μg mL ⁻¹)	Ionisation mode	Molecular mass (Da)	Retention time (RT, min)
	LC			
Beflubutamid-d ₇	0.5	+/-	362.1635	16.74
Metsulfuron-d ₃	0.5	+/-	384.0931	10.66
Succinic acid-d ₄	5	_	122.0517	0.94
Nonanedioic acid-d ₁₄	5	_	202.1927	10.41
¹³ C-Sulfamethazine	5	+	293.2900	7.24
	GC			
9,10-Anthraquinone-d ₈	1		216.1026	20.60
1-Nitronaphthalene-d ₇	1		180.0916	16.60
Benzo[g,h,i]perylene-d ₁₂	1		288.1692	30.56
Pentadecane-d ₃₂	0.05		244.4513	14.99
Pentacosane-d ₅₂	1		404.7333	24.81
Naphthalene-d ₈	0.1		136.1128	11.04
2,2',5,5'-tetrachlorobiphenyl ¹³ C ₁₂ (PCB52*)	0.05		301.9626	20.29
Perylene-d ₁₂	1		264.1692	28.18

Table S6. Injection internal standard solutions with molecular mass and retention time.

Internal standard	Ionisation mode	Molecular mass (Da)	Retention time (RT, min)			
LC						
Simazine-d ₁₀	+	211.1409	11.95			
Diuron-d ₆	+/-	238.0547	13.69			
¹³ C-Diclofenac	+/-	301.0368	15.61			
		GC				
9-Fluorenone-d ₉		212.1410	18.16			
Phenanthrene d ₁₀		188.1410	18.5			

Table S7. Chromatographic elution gradient for LC-HRMS.

Time (min)	Mobile phase A (%)	Mobile phase B (%)
0	98	2
2	98	2
9	60	40
20	2	98
25	2	98

Table S8. QToF parameters for both ionization modes used.

		ESI (+)	ESI (-)
	Sheath gas temperature (°C)	300	300
	Sheath gas flow (L/min)	13	13
Course never eters	Nebulization pressure (psig)	30	30
Source parameters	Capillary tension (V)	3500	3500
	Auxiliary gas temperature (°C)	200	200
	Auxiliary gas flow (L/min)	15	15
	Mass range (m/z)	70-3200	70-3200
	Calibration references	121.0508; 922.0098	112.9855; 1033.9881
A aquisition navometers	Scan number (spectra/min)	4	4
Acquisition parameters		Funnel Exit DC: 50	Funnel Exit DC: 50
	IFunnel (V)	Funnel RF HP: 200	Funnel RF HP: 200
		Funnel RF LP: 100	Funnel RF LP: 100

Table S9. GC-QToF operating conditions.

	Parameters	EI	NICI
	Injection type	Pulsed sp	litless
	Injection pulse pressure (psi)	50	
	Injection temperature (°C)	300	
GC	Carrier gas flow rate (He, mL min ⁻¹)	1.2	
	Transfer line temperature (°C)	280)
	Quench gas flow rate (He, mL min ⁻¹)	4	
	Gas collision flow rate (N ₂ , mL min ⁻¹)	1	
	Initial temperature (°C); hold time (min)	40; 1.8	
Oven nuceuemmine	Temperature rate (°C min ⁻¹)	10	
Oven programming	Final temperature (min); hold time (min)	325;	10
	Total (min)	40.3	3
	Ionisation energy (eV)	70	70
	Source temperature (°C)	280	70
QToF	Solvent delay (min)	6.5	185
	Reactant gas -		- CH ₄ (99.999%)
	Mass range (m/z)	20-600	-

4 Quality assurance and controls

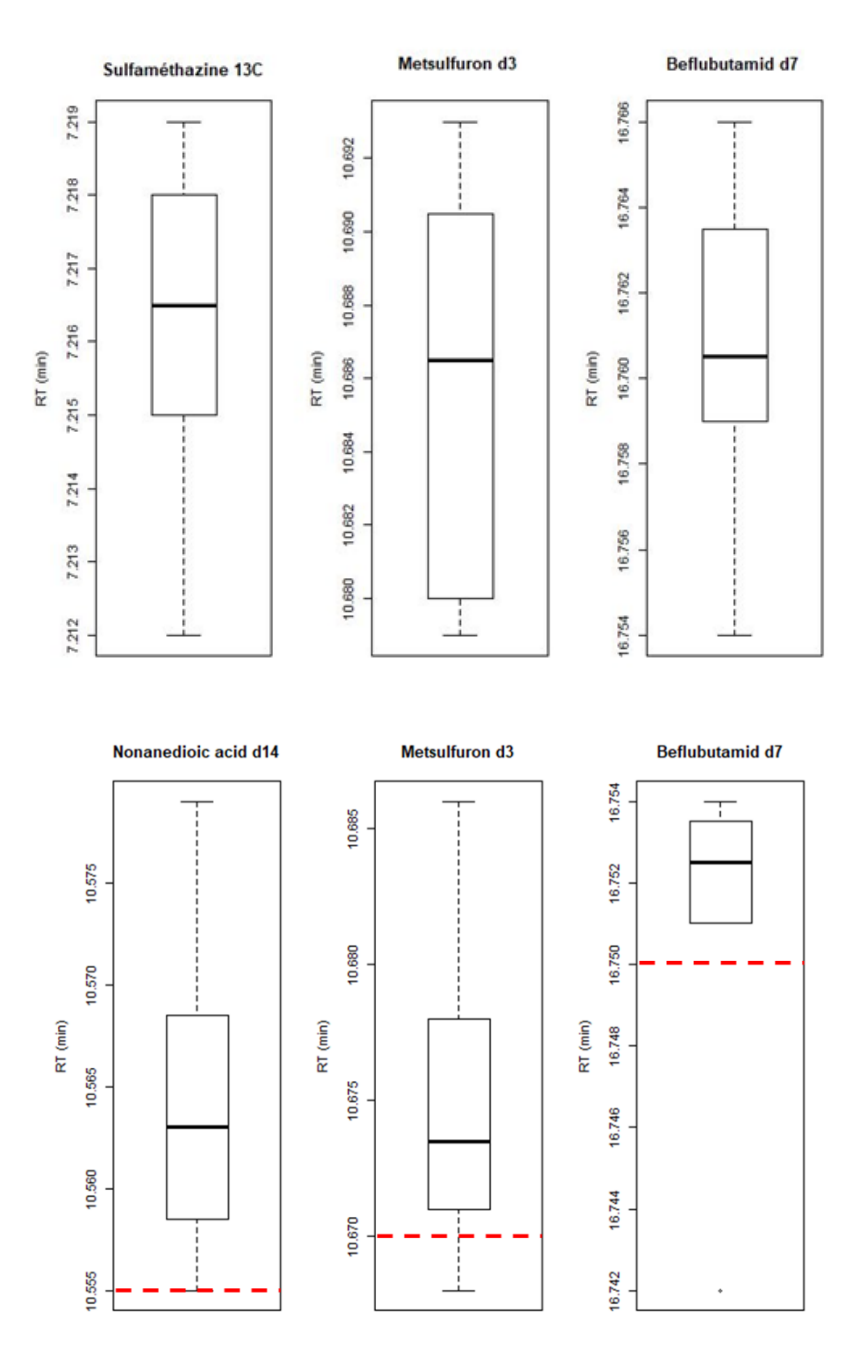


Figure S1. Variation of the monoisotopic ion retention time in QC samples of different internal standards of extraction (EIS) in ESI (+) (top) and ESI (-) (bottom) modes during sample analysis by LC-QToF. The retention time values of these compounds (corresponding to the analysis of the analytical standard for this substance) are represented by the red lines. Note they are out of the range for ¹³C-sulfamethazine (7.425 min), metsulfuron-d₃ (16.670 min) and beflutamid-d₇ (16.750 min) in ESI (+).

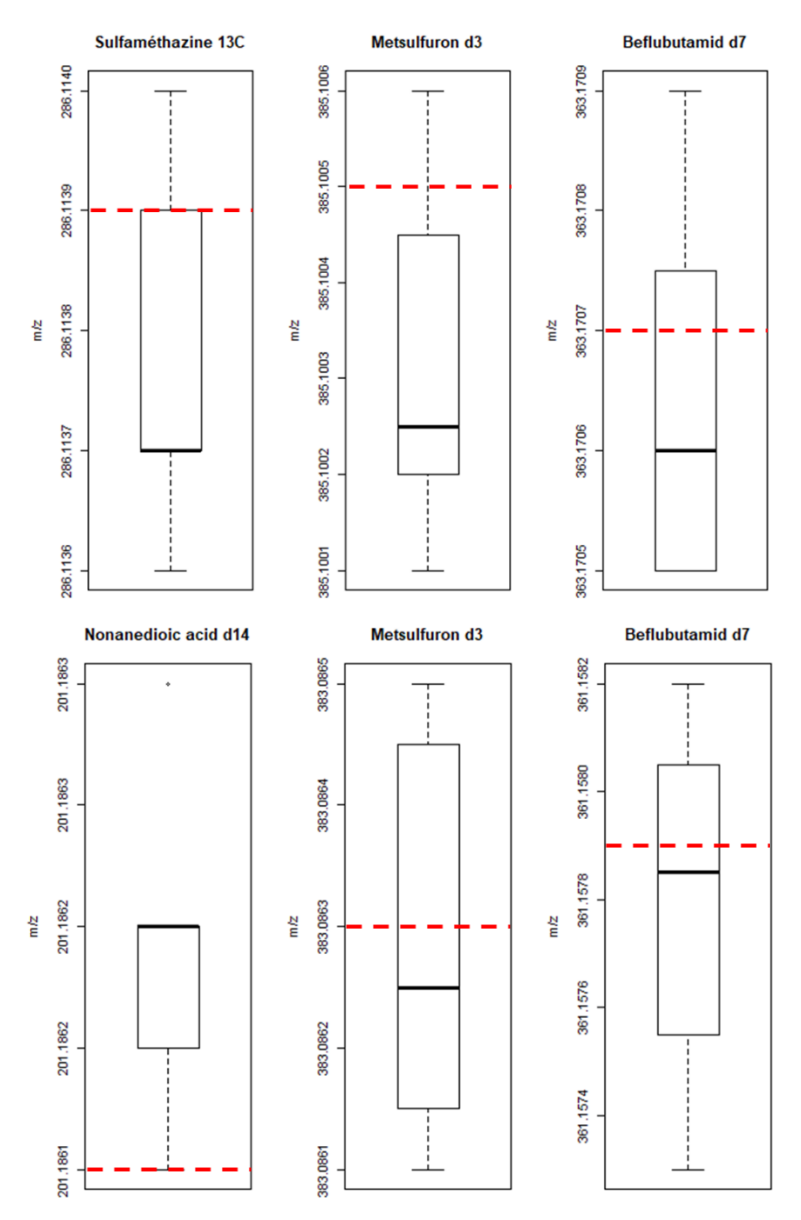


Figure S2. Variation of the monoisotopic ion mass-to-charge ratio (m/z) in QC samples of different extraction internal standards (EIS) in ESI (+) (top) and ESI (-) (bottom) mode during sample analysis by LC-QToF. The values of the ionized molecular weights are represented by the red lines.

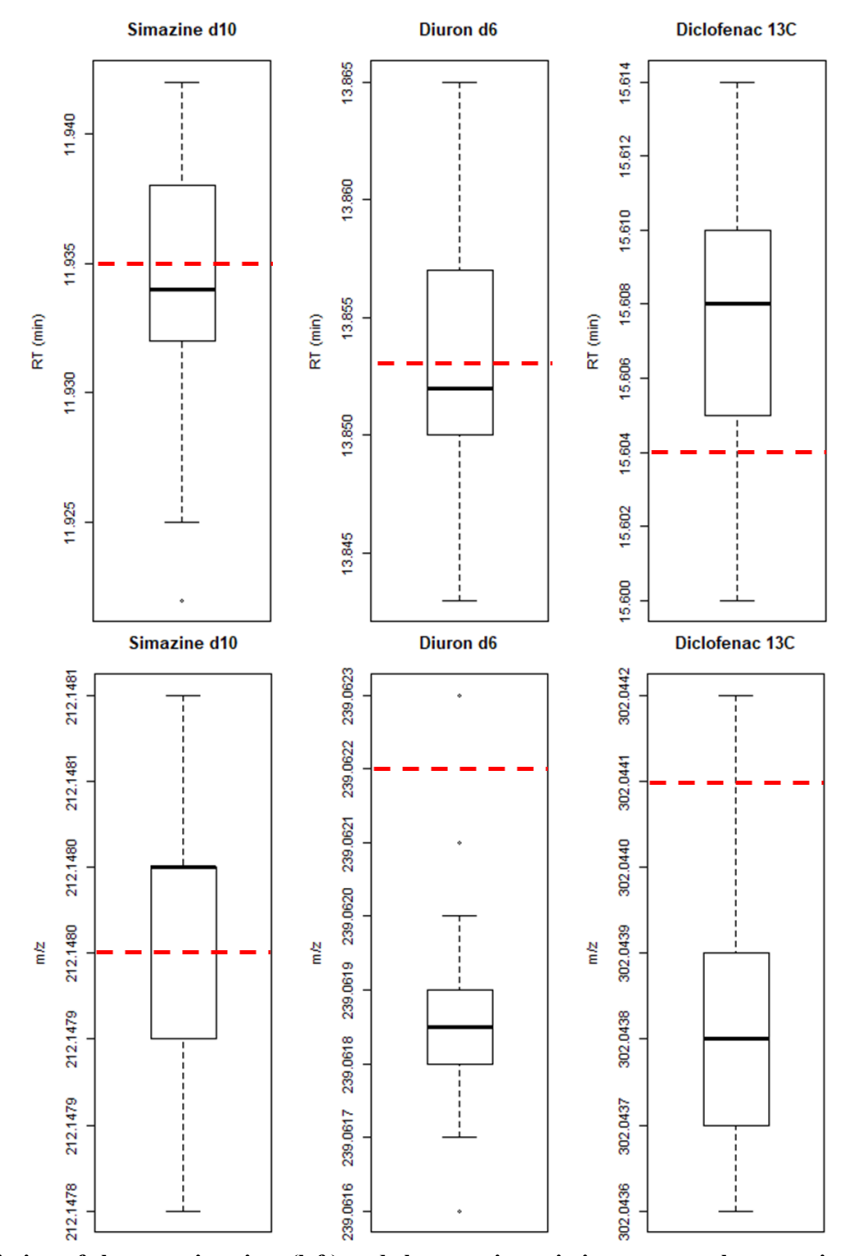


Figure S3. Variation of the retention time (left) and the monoisotopic ion mass-to-charge ratio (m/z) (right) in QC samples of different injection internal standards (IIS) in ESI (+) mode during sample analysis by LC-QToF. The values of the ionized molecular weights are represented by the red lines.

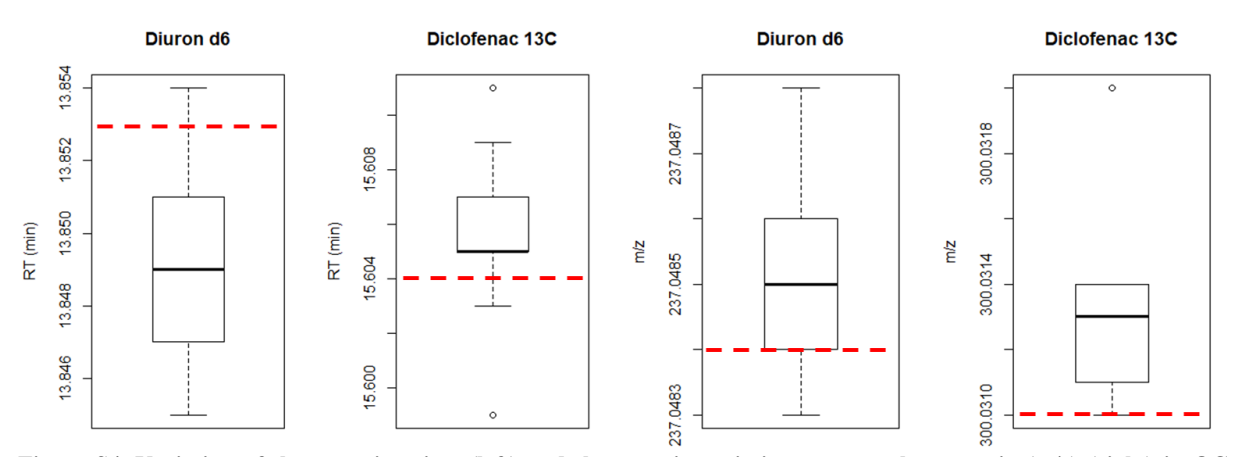


Figure S4. Variation of the retention time (left) and the monoisotopic ion mass-to-charge ratio (m/z) (right) in QC samples of different injection internal standards (IIS) in ESI (–) mode during sample analysis by LC-QToF. The values of the ionized molecular weights are represented by the red lines.

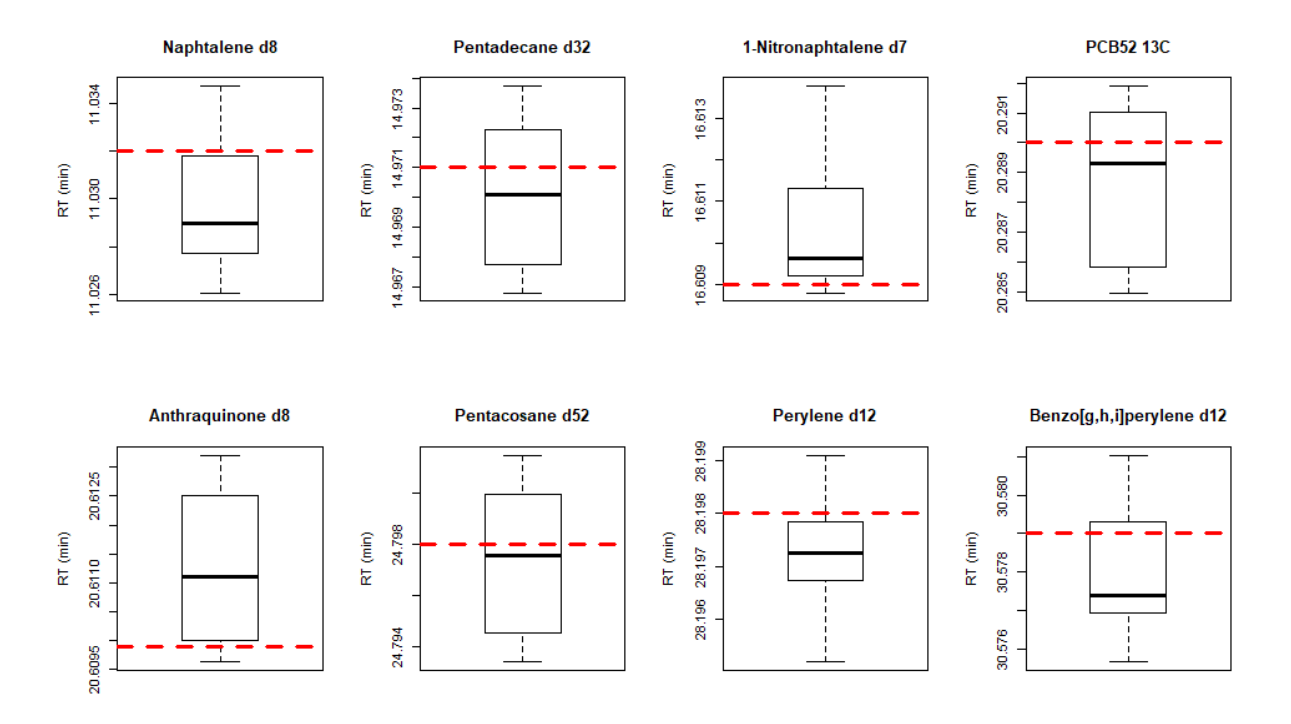


Figure S5. Variation of the retention time in QC samples of different injection internal standards (EIS) during sample analysis by GC-QToF. The values of the ionized molecular weights are represented by the red lines.

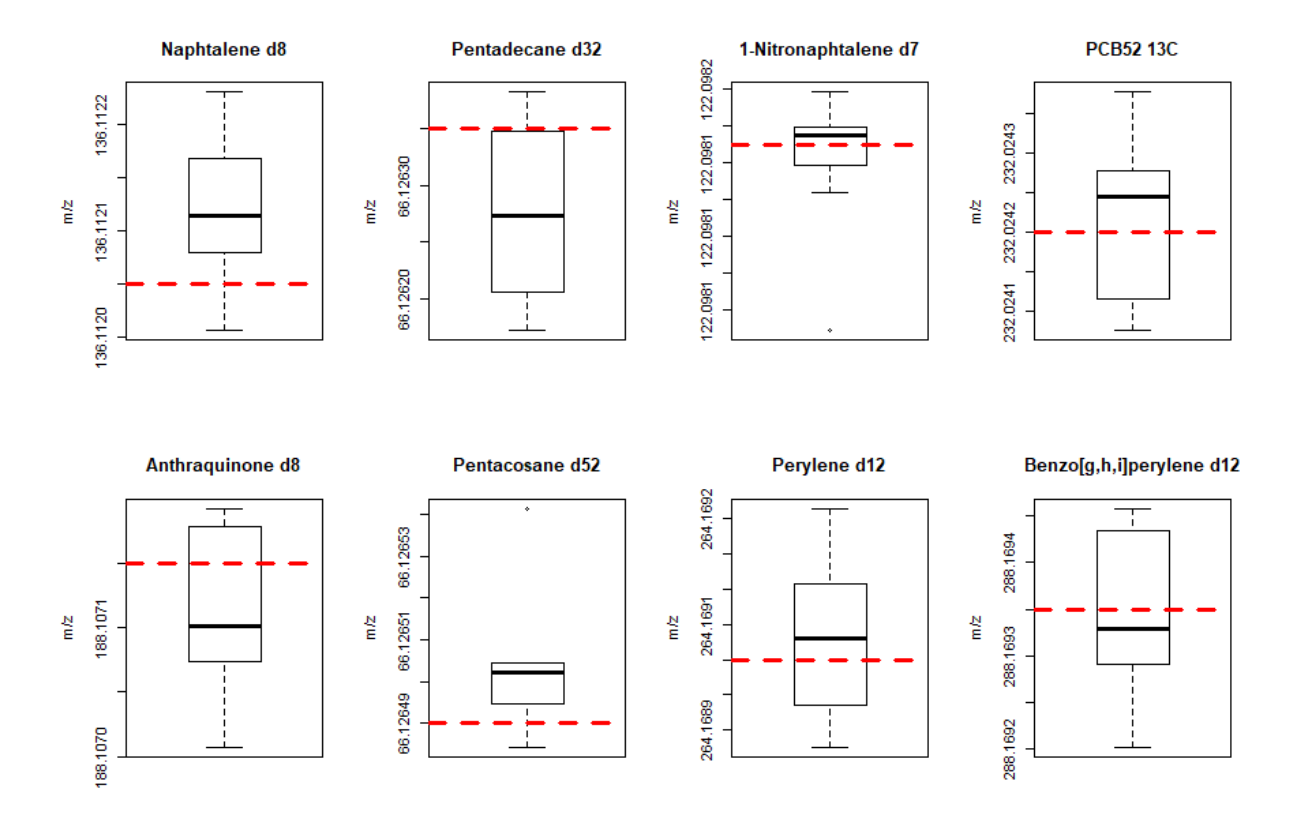


Figure S6. Variation of the monoisotopic ion mass-to-charge ratio (m/z) in QC samples of different injection internal standards (EIS) during sample analysis by GC-QToF. The values of the ionized molecular weights are represented by the red line.

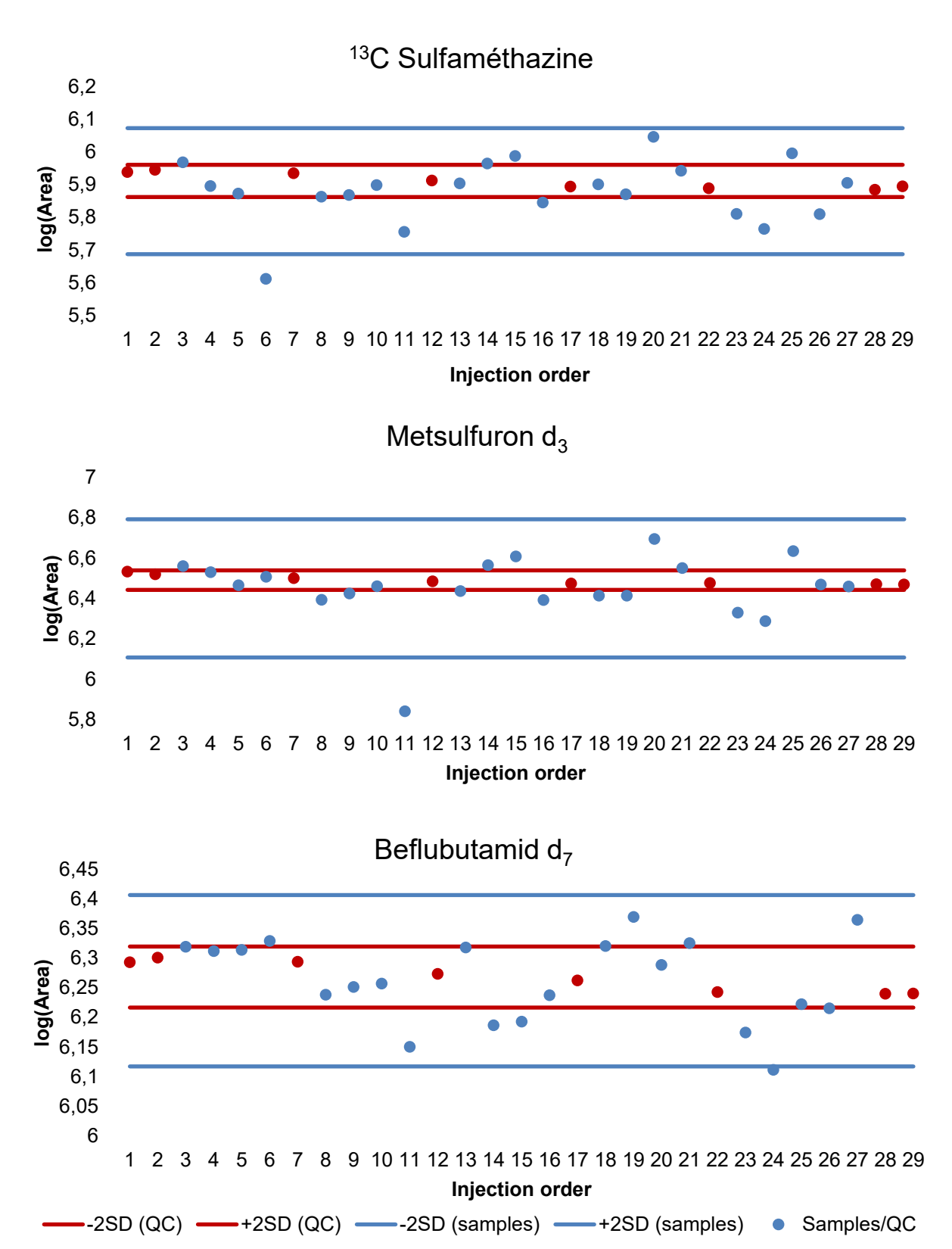


Figure S7. Control chart of areas (log area) observed for three internal extraction standards for QC pool samples (red dots) and vehicular combustion samples (blue dots) according to the injection order during LC-QToF analysis (ESI+). The red and blue lines represent the observed standard deviation (2σ) for all pooled QC and samples respectively.

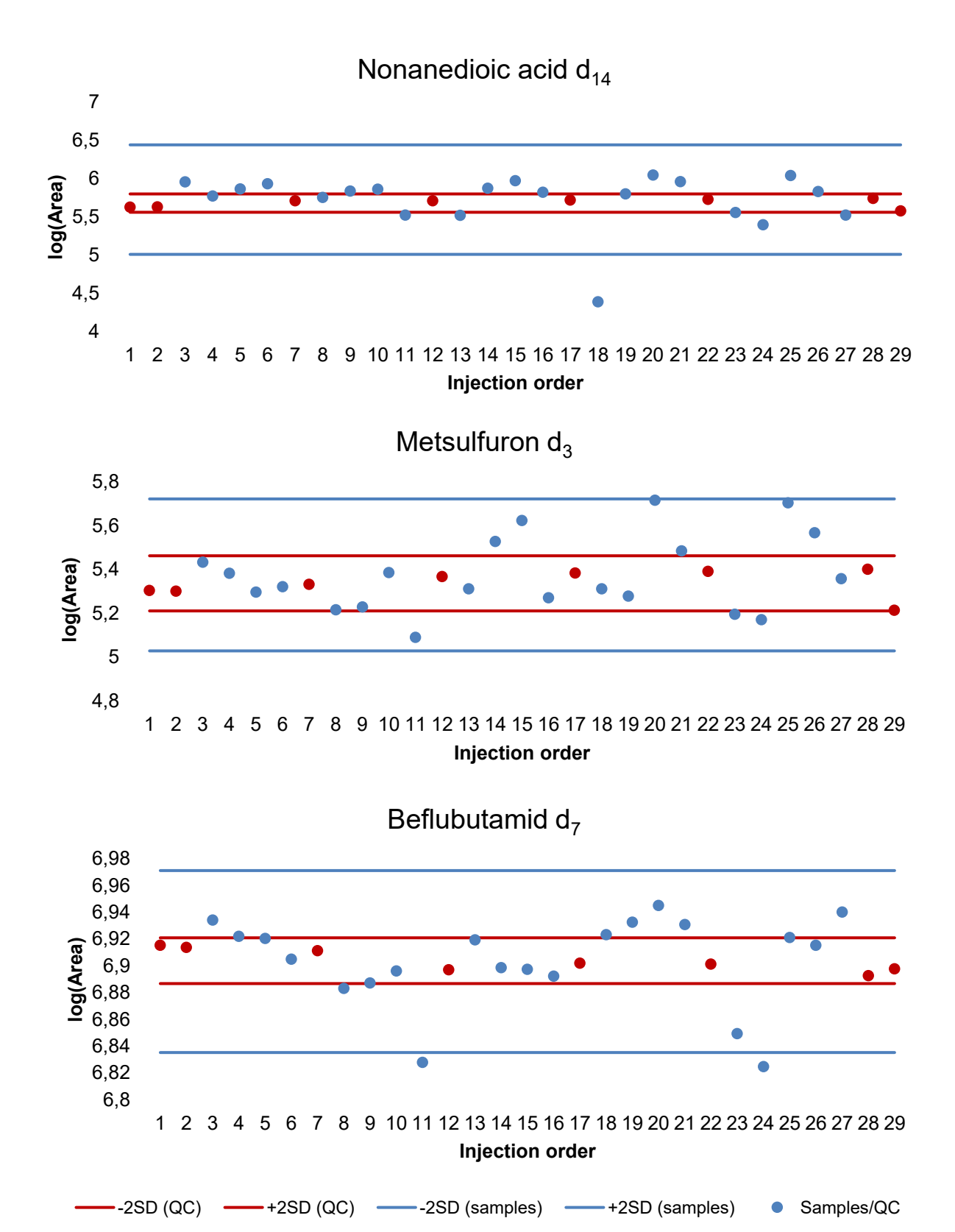


Figure S8. Control chart of areas (log area) observed for three internal extraction standards for QC pool samples (red dots) and vehicular combustion samples (blue dots) according to the injection order during LC-QToF analysis (ESI–). The red and blue lines represent the observed standard deviation (2σ) for all pooled QC and samples respectively.

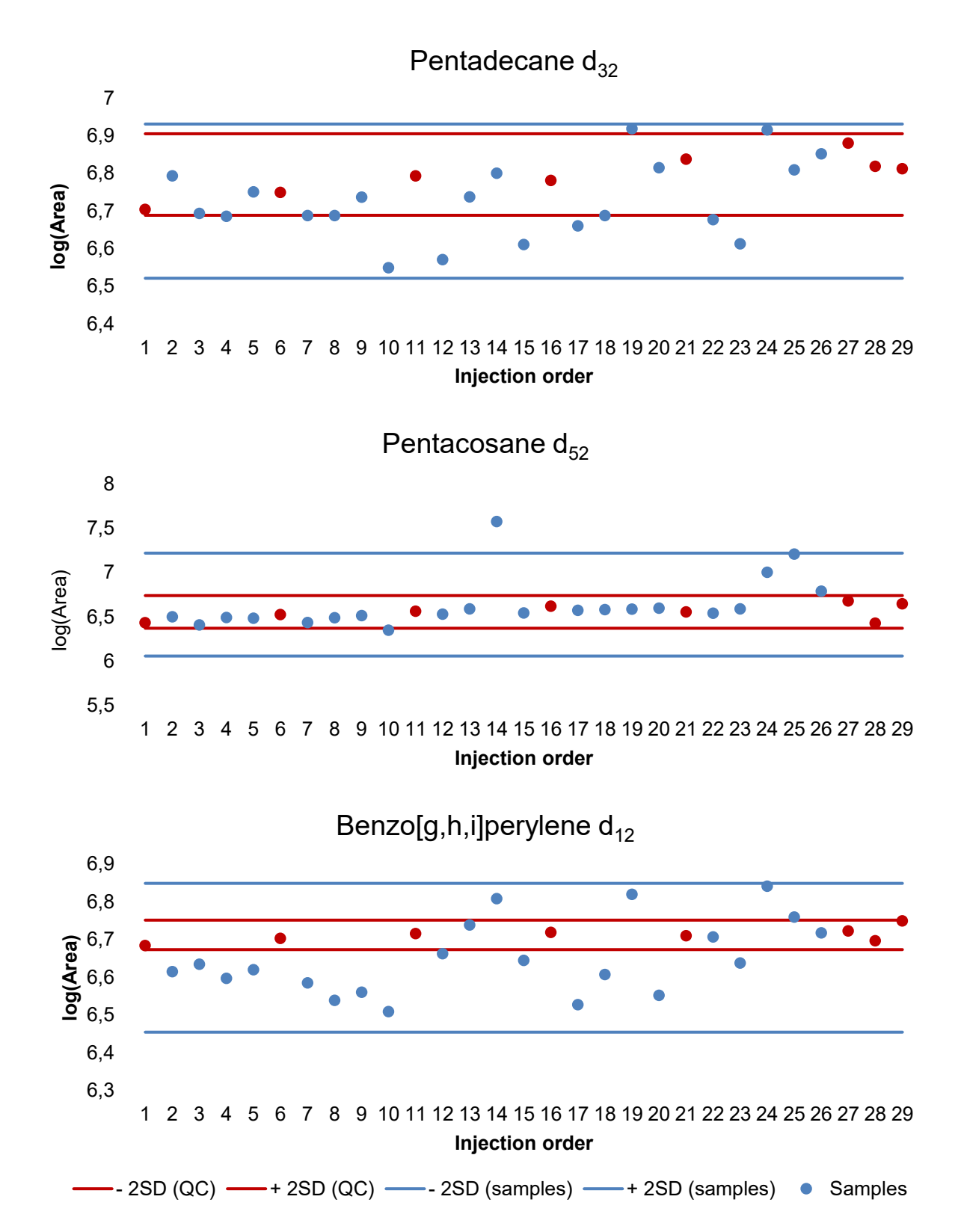


Figure S9. Control chart of areas (log area) observed for three internal extraction standards for QC pool samples (red dots) and vehicular combustion samples (blue dots) according to the injection order during GC-QToF analysis. The red and blue lines represent the observed standard deviation (2σ) for all pooled QC and samples respectively.

5 Data treatment

 $Table \ S10. \ Parameters \ used \ for \ features \ extraction \ with \ the \ RFE \ algorithm \ (Profinder, Agilent \ Technologies) \ with \ the \ number \ of \ detected \ entities \ and \ the \ number \ of \ entities \ retained \ in \ the \ final \ dataset.$

	LC-QToF		GC-QToF	
_	ESI (+)	ESI (-)	HEI	
First step:				
- Minimal height for peaks	25000	20000	40000	
- Binning and alignment:				
 Retention time window 	0.15 min	0.15 min	0.05 min	
 Mass window (LC) 	15 ppm + 2 mDa	15 ppm + 2 mDa	/	
• Dot product (GC)	/	/	0.6	
- Allowed ion species adduct	$\mathrm{H}^{\scriptscriptstyle +}$	H^-		
Second step:				
- Match tolerance				
• RT	$\pm 0.15 \text{ min}$	$\pm 0.15 \text{ min}$	$\pm 0.05 \text{ min}$	
 Mass 	$\pm 10 \text{ ppm}$	$\pm~10~\mathrm{ppm}$		
- Minimal height for peaks	20000	12000	37000	
Number of detected entities	2873	2879	2546	
Number of entities in the final dataset	1833	1779	1088	

6 Overview of the particulate and gaseous emissions of EURO 5 diesel and gasoline vehicles

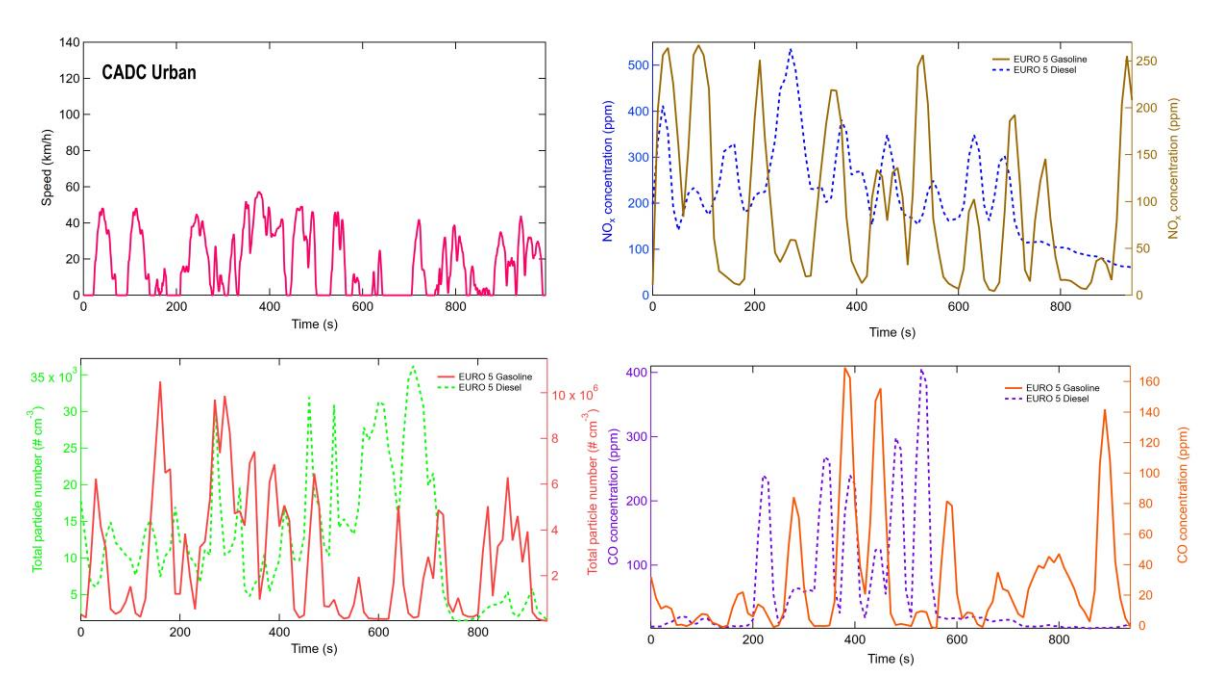


Figure S10. CADC urban speed profile (pink) and time series of the primary particle number (bottom left-corner), NO_x (top right-corner) and CO concentrations (bottom right-corner) at emission for the studied EURO 5 diesel and gasoline vehicles during the hot-start CADC urban driving cycle.

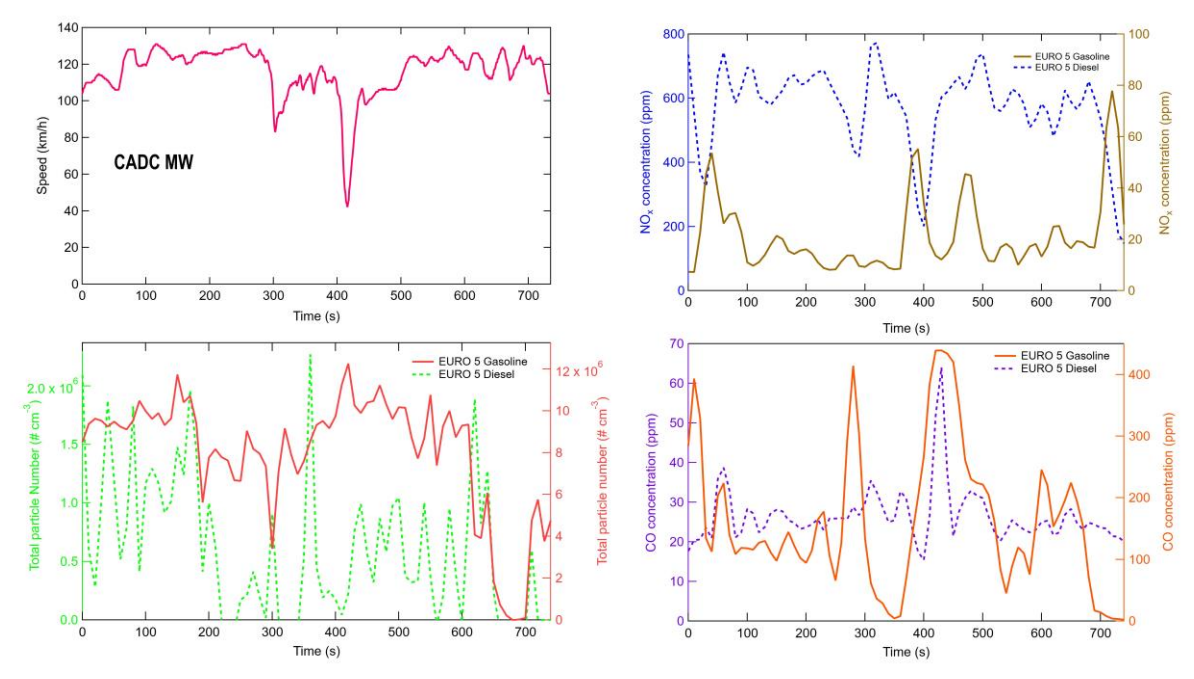


Figure S11. CADC motorway (MW) speed profile (pink) and time series of the primary particle number (bottom left-corner), NO_x (top right-corner) and CO concentrations (bottom right-corner) at emission for the studied EURO 5 diesel and gasoline vehicles during the hot-start CADC motorway driving cycle.

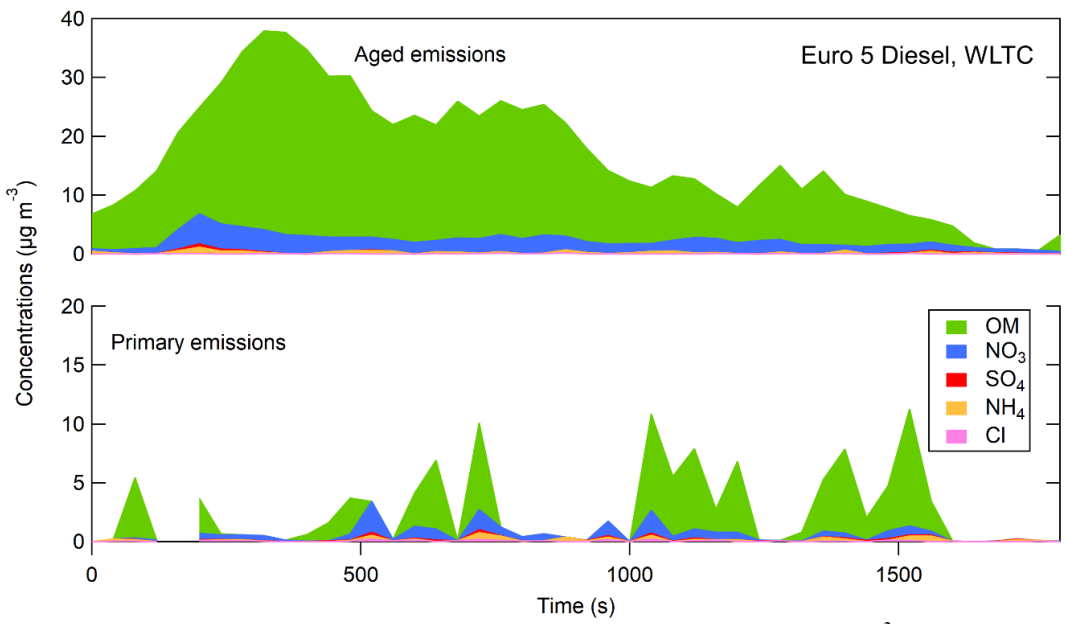


Figure S12. Temporal variations of organics, NO_3 , SO_4 , NH_4 and Cl concentrations ($\mu g \ m^{-3}$) measured by the ACSM for the primary and aged emissions during the ambient start WLTC driving cycle for the EURO 5 diesel vehicle. Concentrations without dilution corrections.

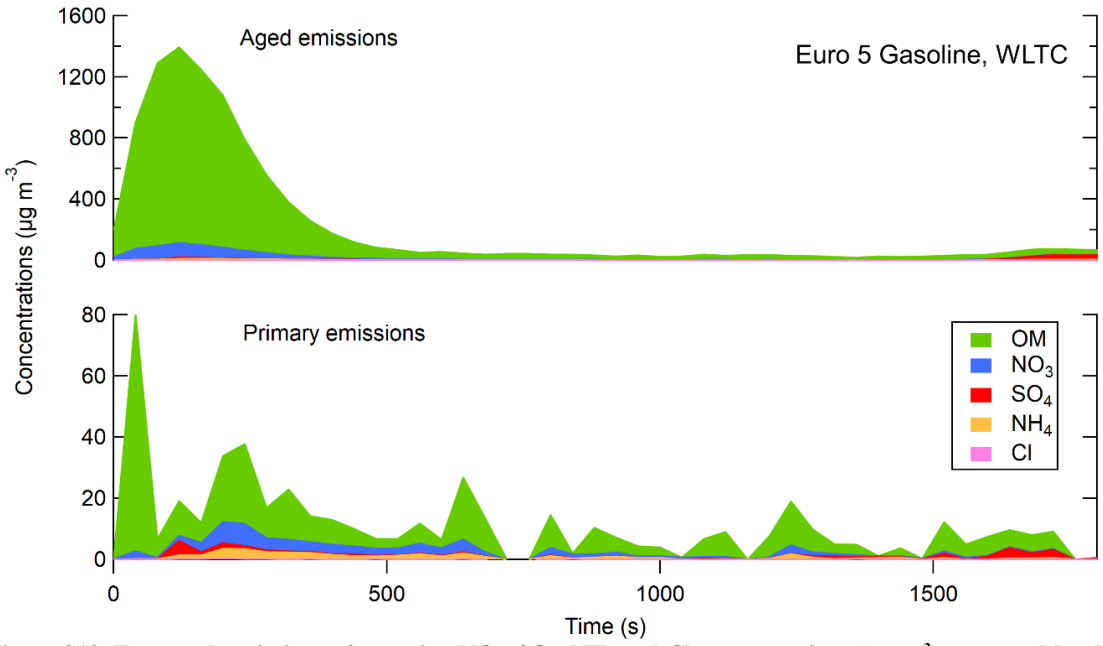


Figure S13. Temporal variations of organics, NO₃, SO₄, NH₄ and Cl concentrations (μ g m⁻³) measured by the ACSM for the primary and aged emissions during the ambient start WLTC driving cycle for the EURO 5 gasoline vehicle. Concentrations without dilution corrections.

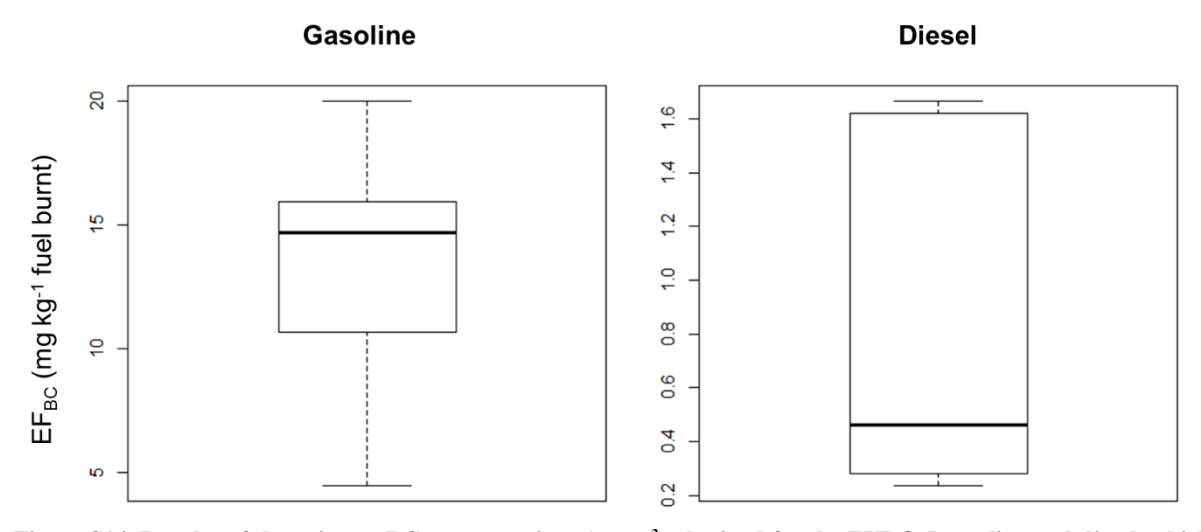


Figure S14. Boxplot of the primary BC concentrations ($\mu g \ m^{-3}$) obtained for the EURO 5 gasoline and diesel vehicles (all driving cycles).

7 Non-target chemical characterization of vehicular OA.

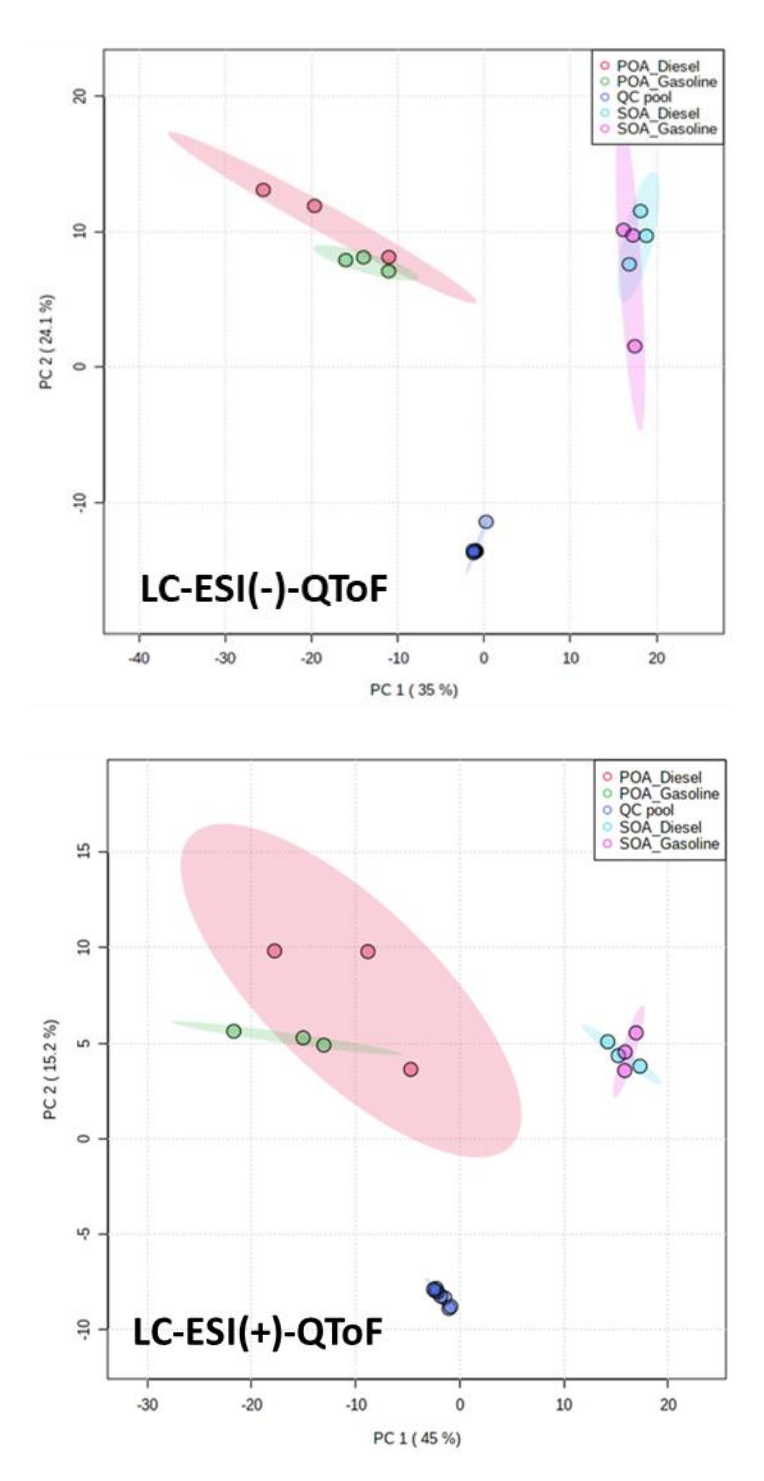


Figure S15. Principal component analysis of samples from primary and secondary vehicular emissions (POA diesel: red, POA gasoline: green, SOA diesel: light blue, SOA gasoline: pink) and pooled QC samples (dark blue). The result is obtained from the NTS analysis performed by LC-QToF (ESI(+) and ESI(-) mode). The data were normalized by pooled QC samples, log-transformed and auto-scaled. The ellipses represent the 95 % confidence zones.

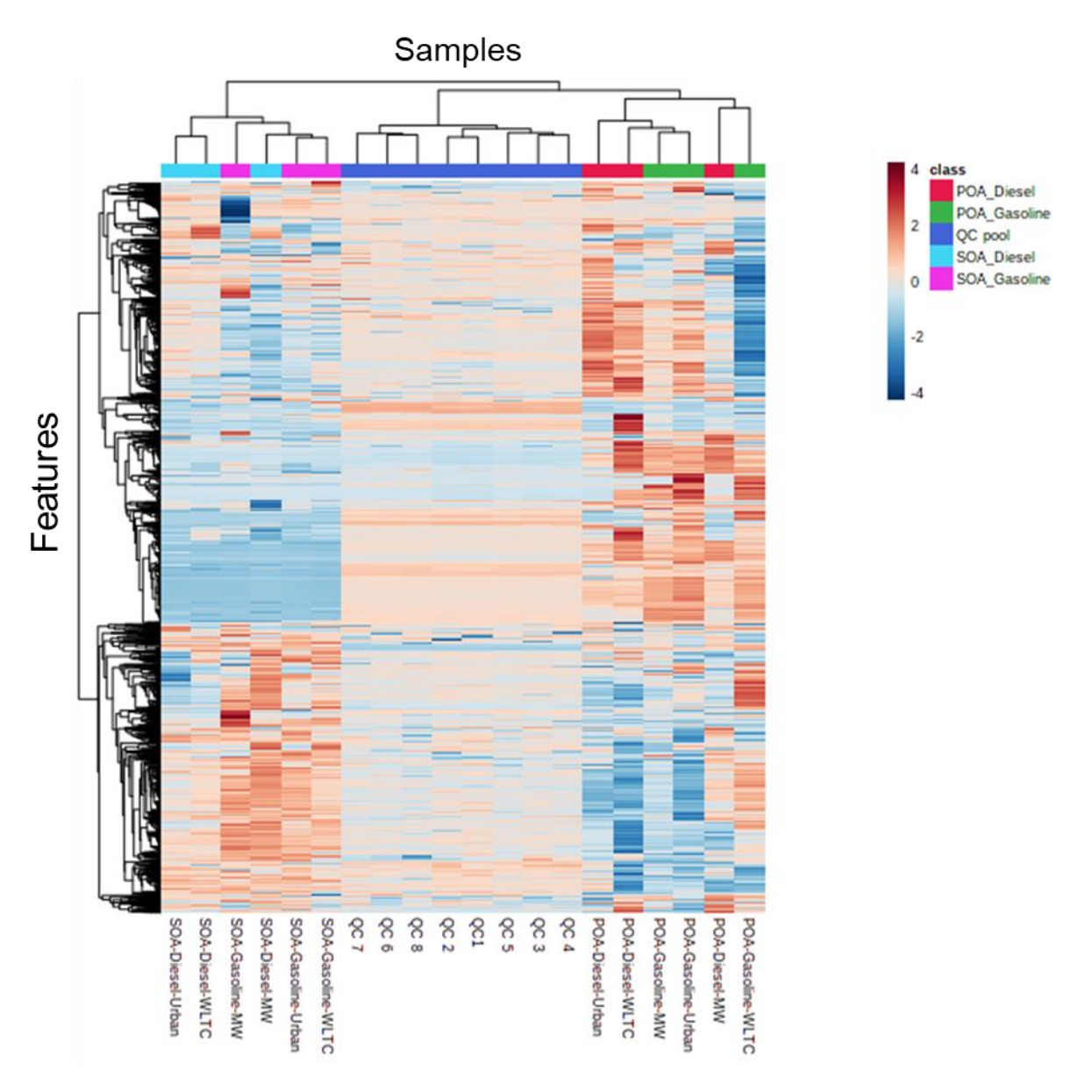


Figure S16. Two-way hierarchical classification and heat map of the different vehicular exhaust samples from LC-QToF analysis in ESI(+) mode. This classification was performed based on the Pearson correlation coefficient using the average linkage method. The colour-scale on the right represented the feature relative abundance in each sample compared to the others.

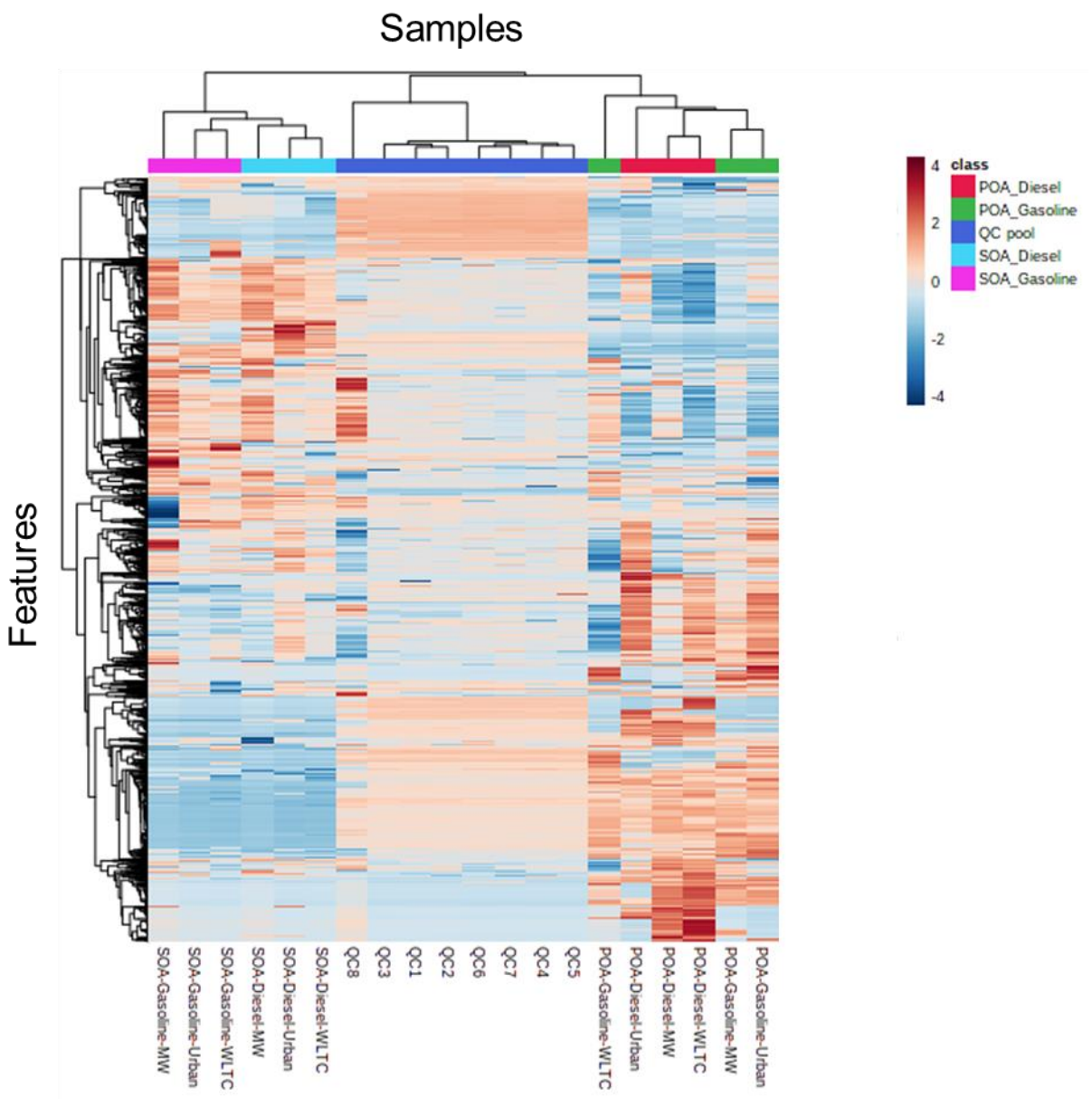


Figure S17. Two-way hierarchical classification and heat map of the different vehicular exhaust samples from LC-QToF analysis in ESI(-) mode. This classification was performed based on the Pearson correlation coefficient using the average linkage method. The colour-scale on the right represented the feature relative abundance in each sample compared to the others.

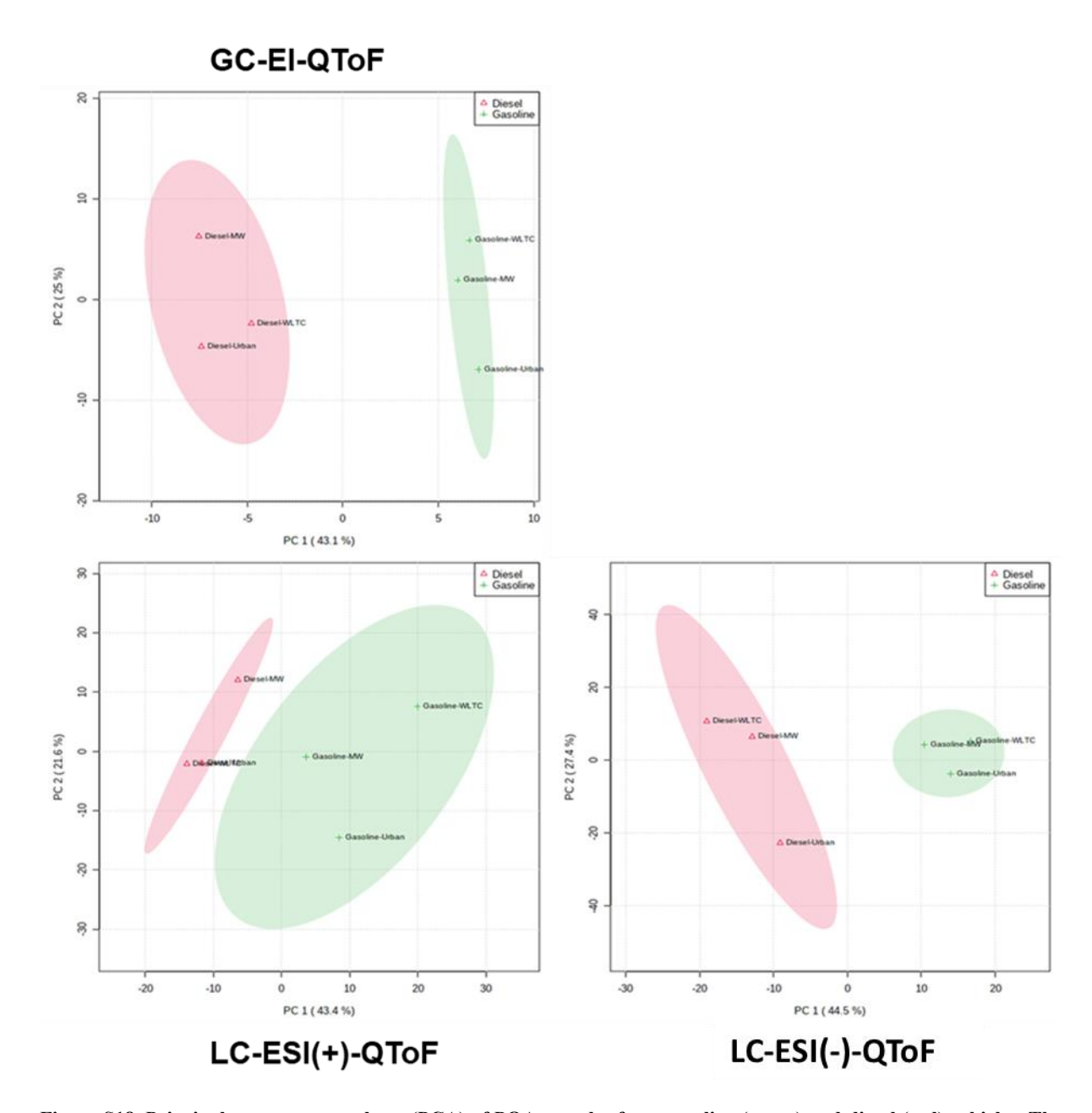


Figure S18. Principal component analyses (PCA) of POA samples from gasoline (green) and diesel (red) vehicles. The results are obtained from the GC-QToF and LC-QToF data and were normalized by pooled QC samples, log-transformed and auto-scaled. The ellipses represent the 95 % confidence zones.

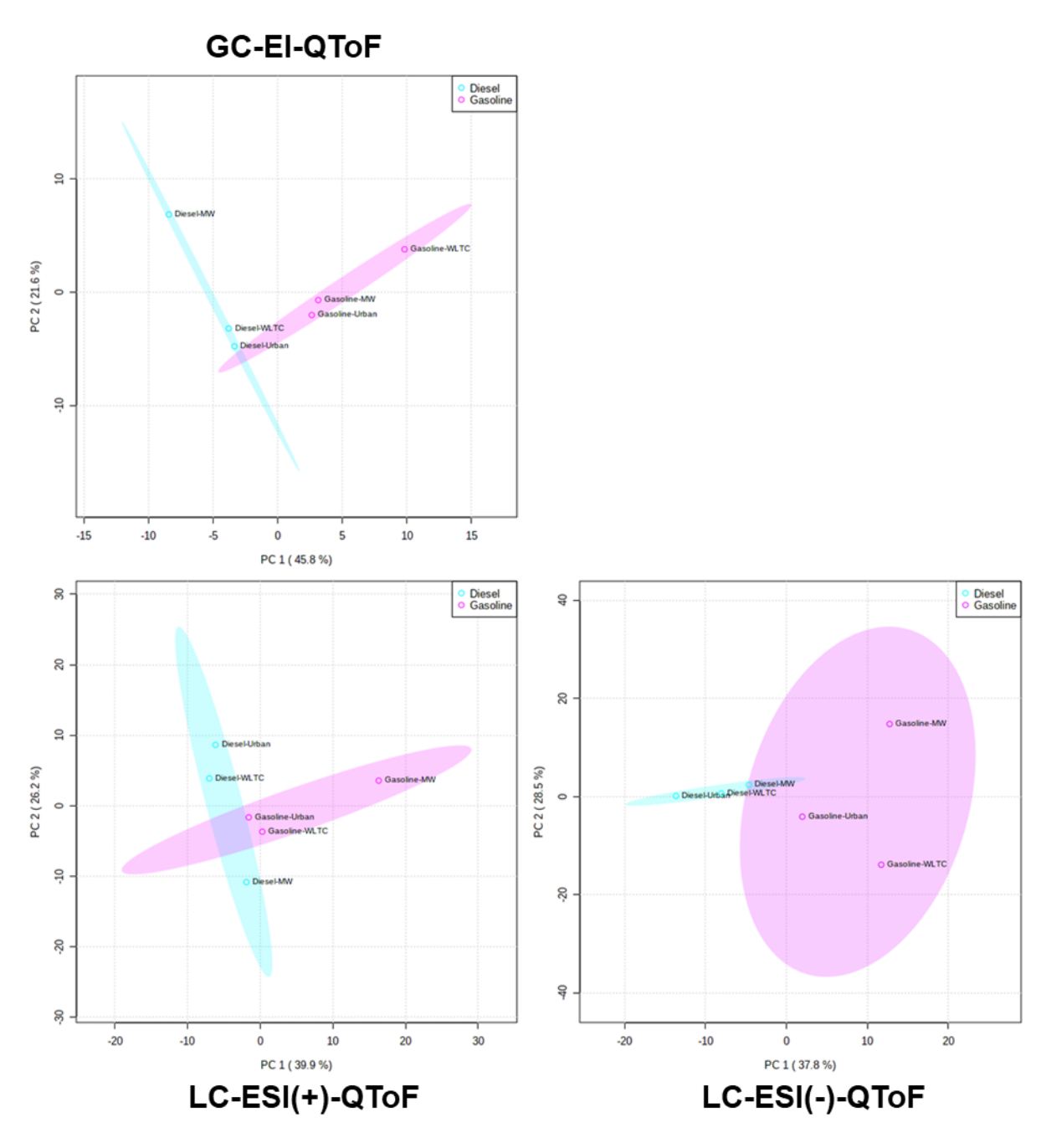
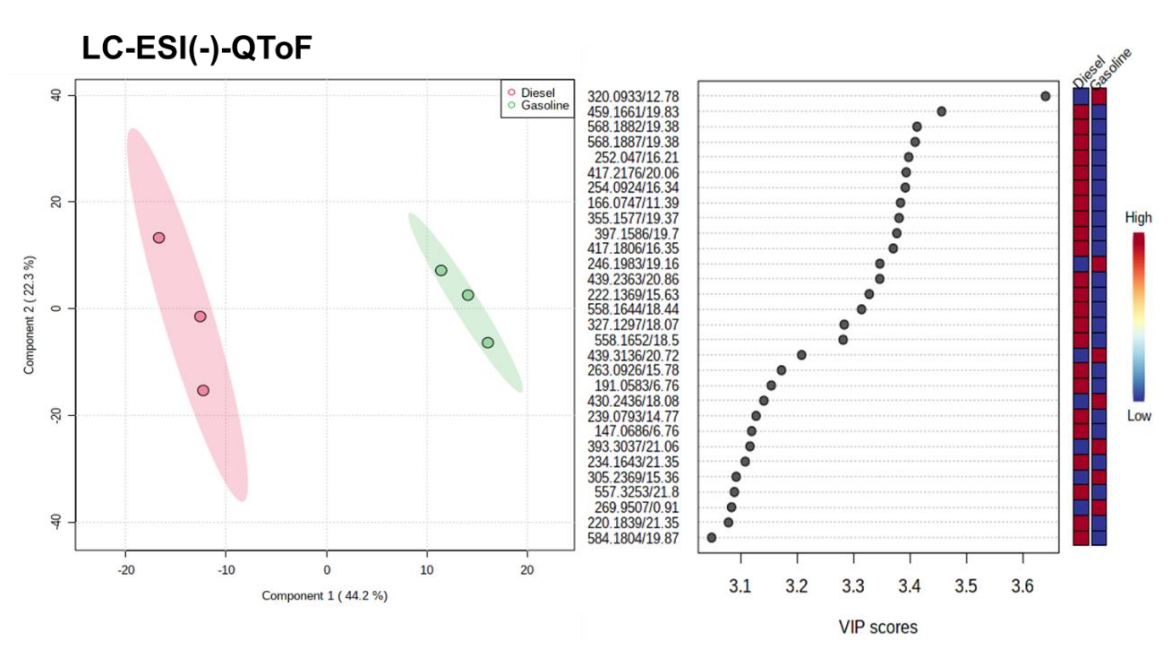


Figure S19. Principal component analyses (PCA) of SOA samples from gasoline (pink) and diesel (light blue) vehicles. The results are obtained from the GC-QToF and LC-QToF data and were normalized by pooled QC samples, log-transformed and auto-scaled. The ellipses represent the 95 % confidence zones.

Table S11. R2 and Q2 values of the explanatory PLS-DA model

OA fraction	Analysis	R²	Q²
	GC-QToF	0.99	0.83
POA	LC-ESI(+)-QToF	0.97	0.65
	LC-ESI(-)-QToF	0.98	0.70
	GC-QToF	0.99	0.83
SOA	LC-ESI(+)-QToF	1.00	0.30
	LC-ESI(-)-QToF	0.98	0.50



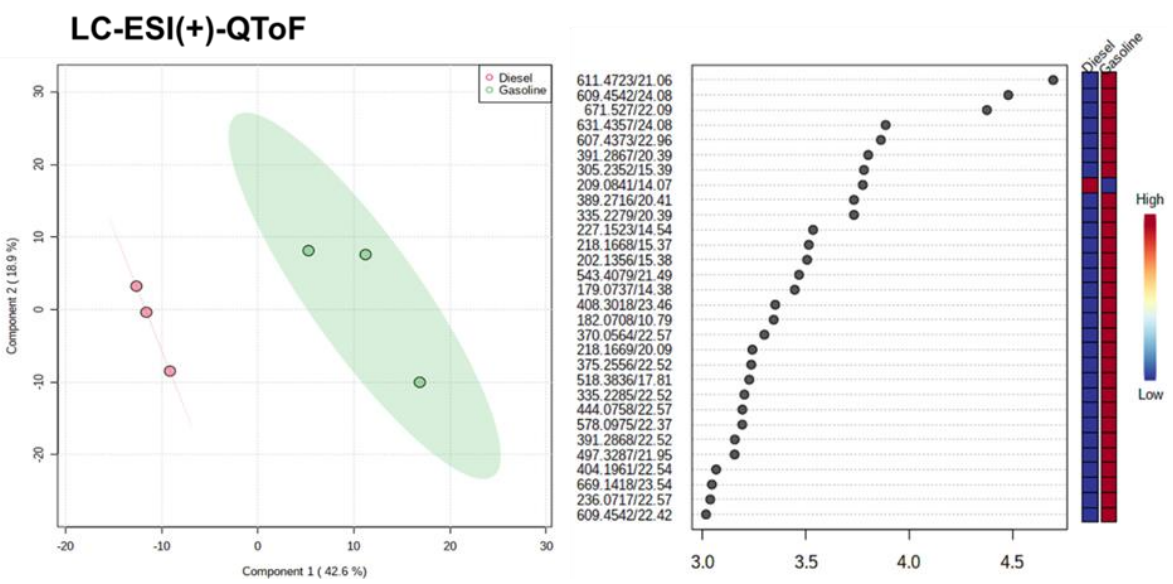


Figure S20. Partial Least Square–Discriminant Analysis (PLS-DA) of POA samples from gasoline and diesel vehicles. The results are obtained from the GC-QToF and LC-QToF (both positive and negative mode) data and were normalized by pooled QC samples, log-transformed and auto-scaled. The ellipses represent the 95 % confidence zones. Classification of chemical entities (left scale: molecular mass/retention time) characteristic of each vehicular source according to the VIP score are displayed on the right. The colour scale indicates the variation in abundance of the chemical entity (100 % = red, 0 % = blue) in all samples of both vehicles. Only the first 30 chemical entities with the highest VIP scores are shown on the graph.

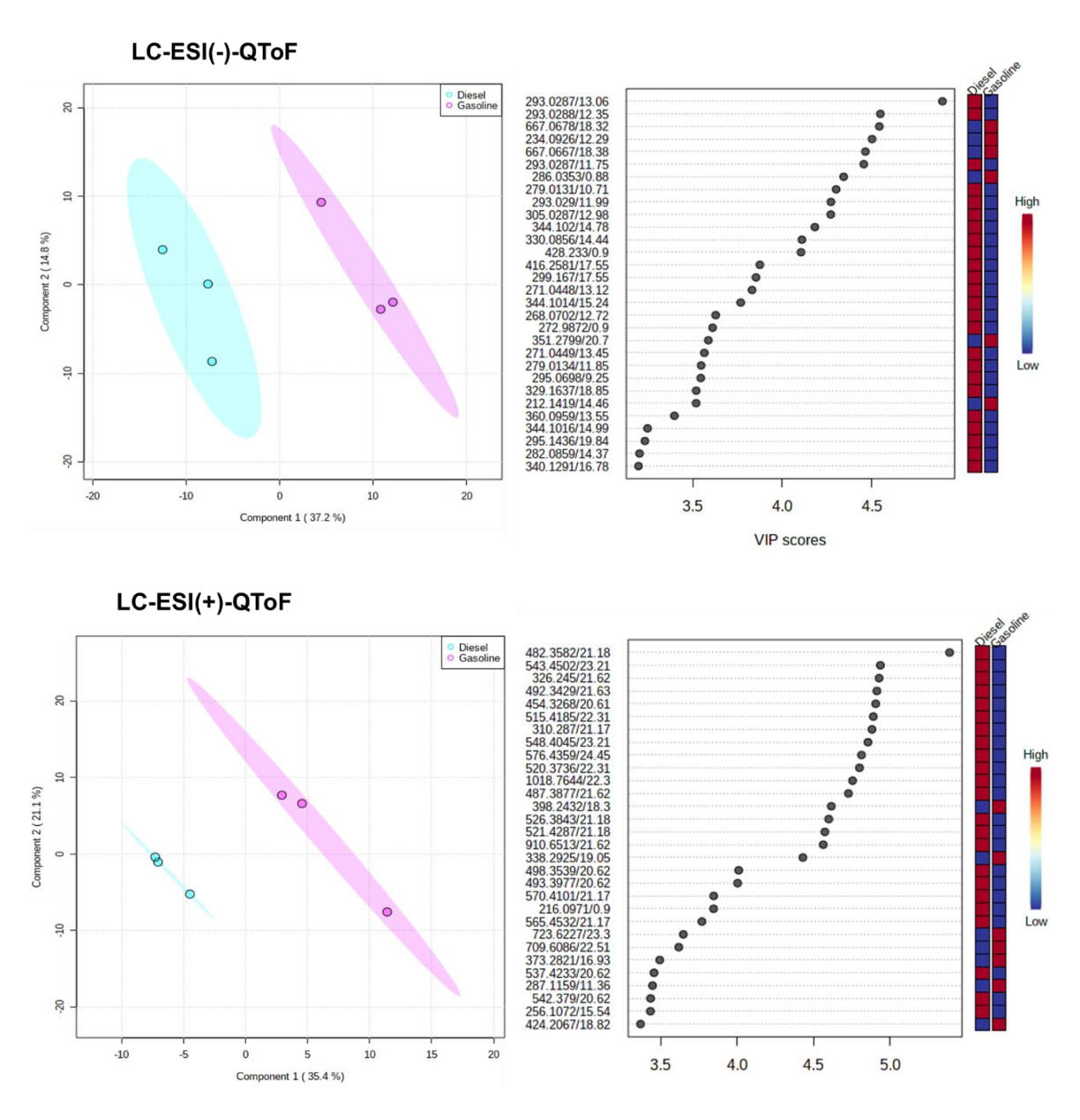


Figure S21. Partial Least Square–Discriminant Analysis (PLS-DA) of SOA samples from gasoline and diesel vehicles. The results are obtained from the GC-QToF and LC-QToF (positive and negative mode) data and were normalized by pooled QC samples, log-transformed and auto-scaled. The ellipses represent the 95 % confidence zones. Classification of chemical entities (left scale: molecular mass /retention time for LC) characteristic of each vehicular source according to the VIP score are displayed on the right. The colour scale indicates the variation in abundance of the chemical entity (100 % = red, 0 % = blue) in all samples of both vehicles. Only the first 30 chemical entities with the highest VIP scores are shown on the graph.

8 Some examples of chromatographic responses of markers.

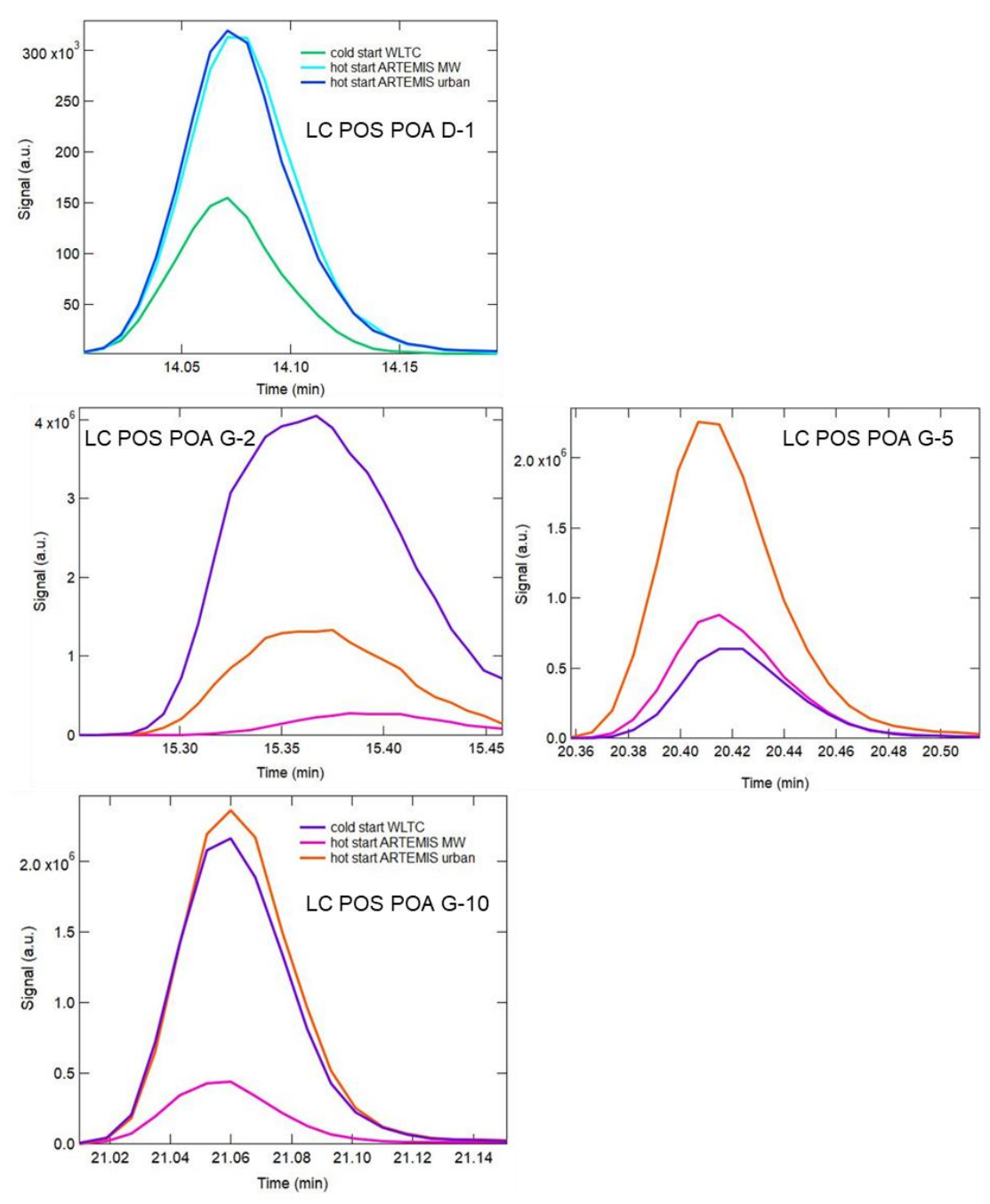


Figure S22. Potential molecular markers characteristic of diesel and gasoline POA from LC-QToF data in positive mode (ESI+). Chromatographic response observed for selected markers in ambient start WLTC, hot-start CADC motorway (MW) and urban driving conditions.

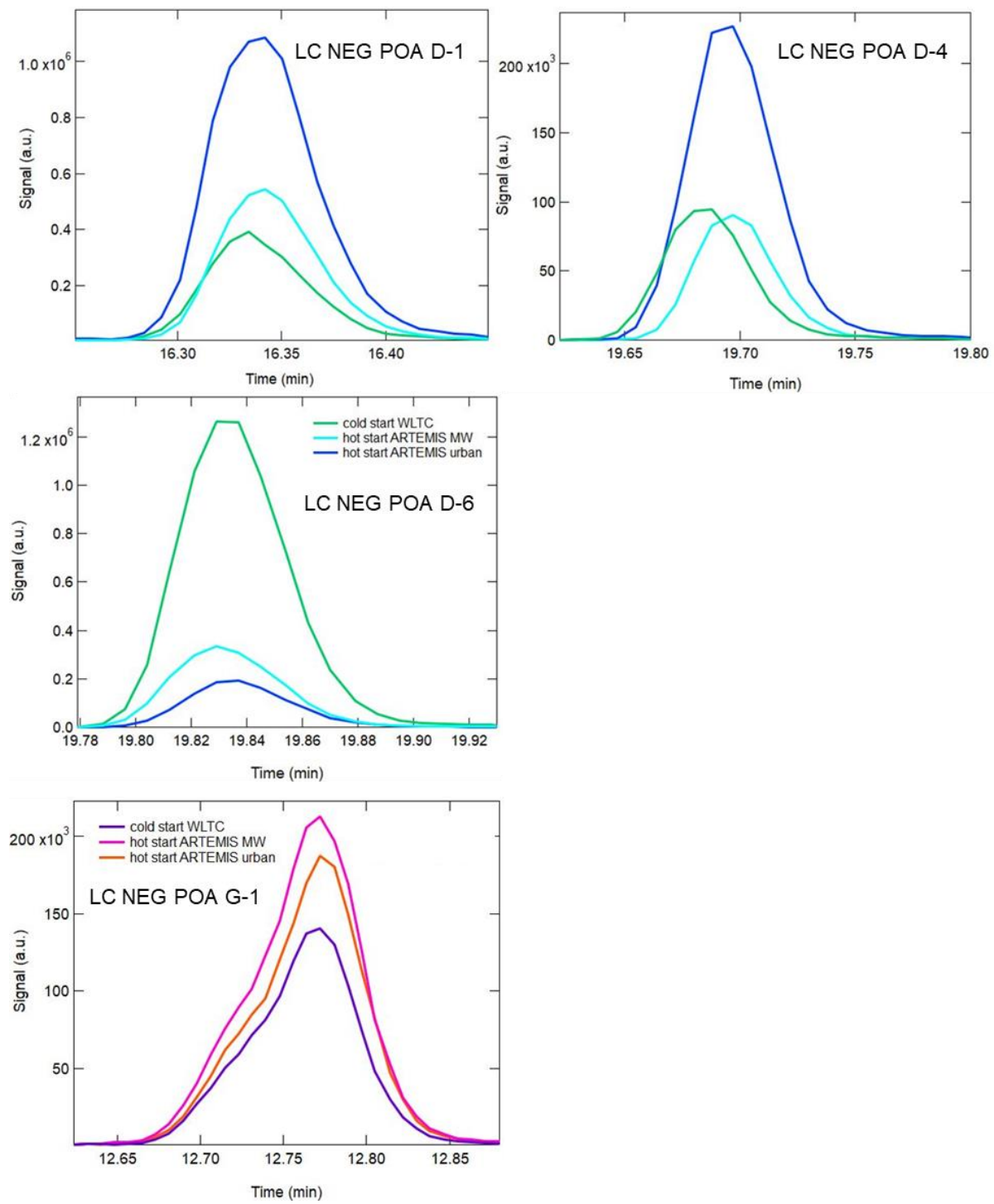


Figure S23. Potential molecular markers characteristic of diesel and gasoline POA from LC-QToF data in negative mode (ESI-). Chromatographic response observed for selected markers in ambient start WLTC, hot-start CADC motorway (MW) and urban driving conditions.

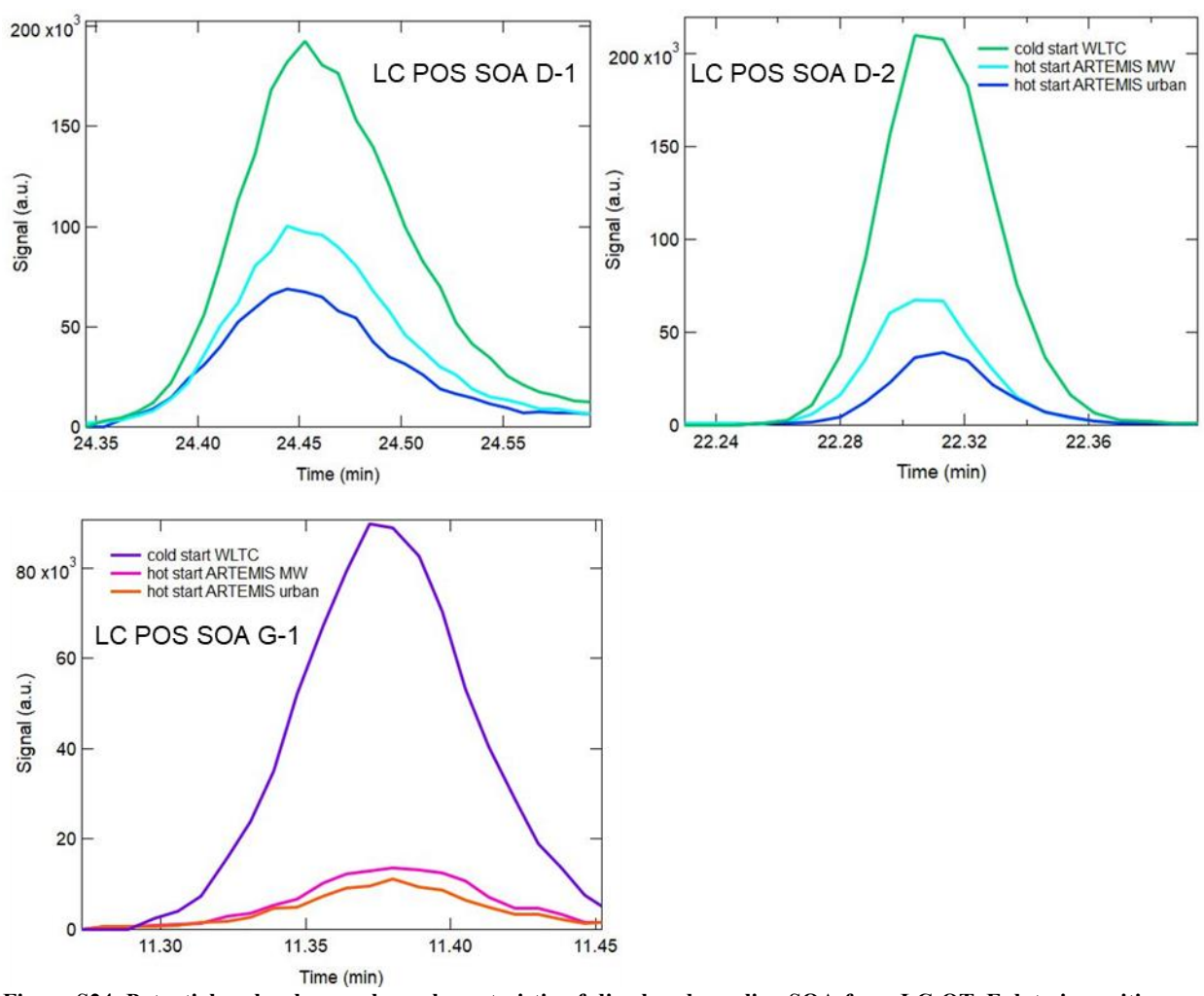


Figure S24. Potential molecular markers characteristic of diesel and gasoline SOA from LC-QToF data in positive mode (ESI+). Chromatographic response observed for selected markers in ambient start WLTC, hot-start CADC motorway (MW) and urban driving conditions.

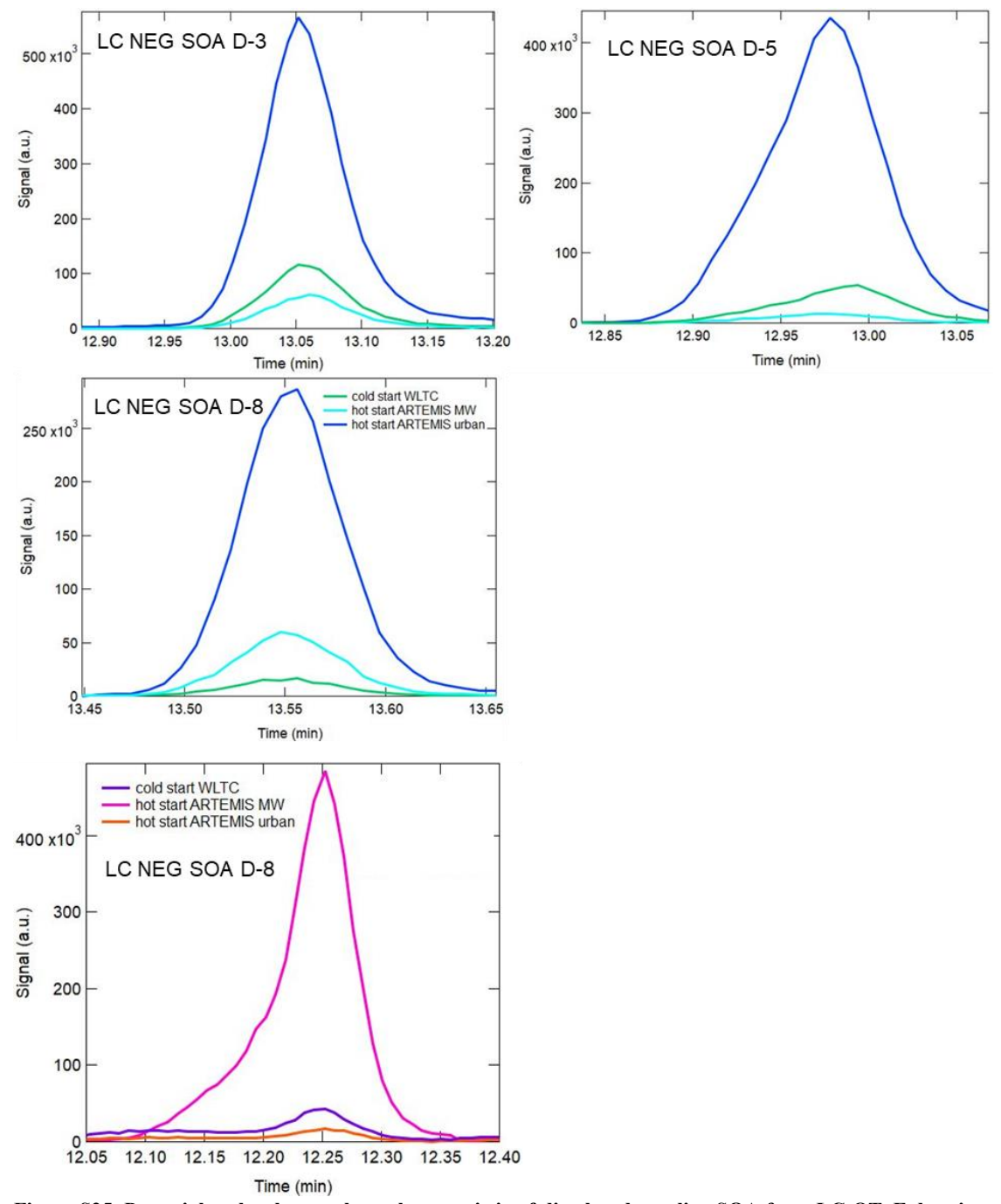


Figure S25. Potential molecular markers characteristic of diesel and gasoline SOA from LC-QToF data in negative mode (ESI-). Chromatographic response observed for selected markers in ambient start WLTC, hot-start CADC motorway (MW) and urban driving conditions.

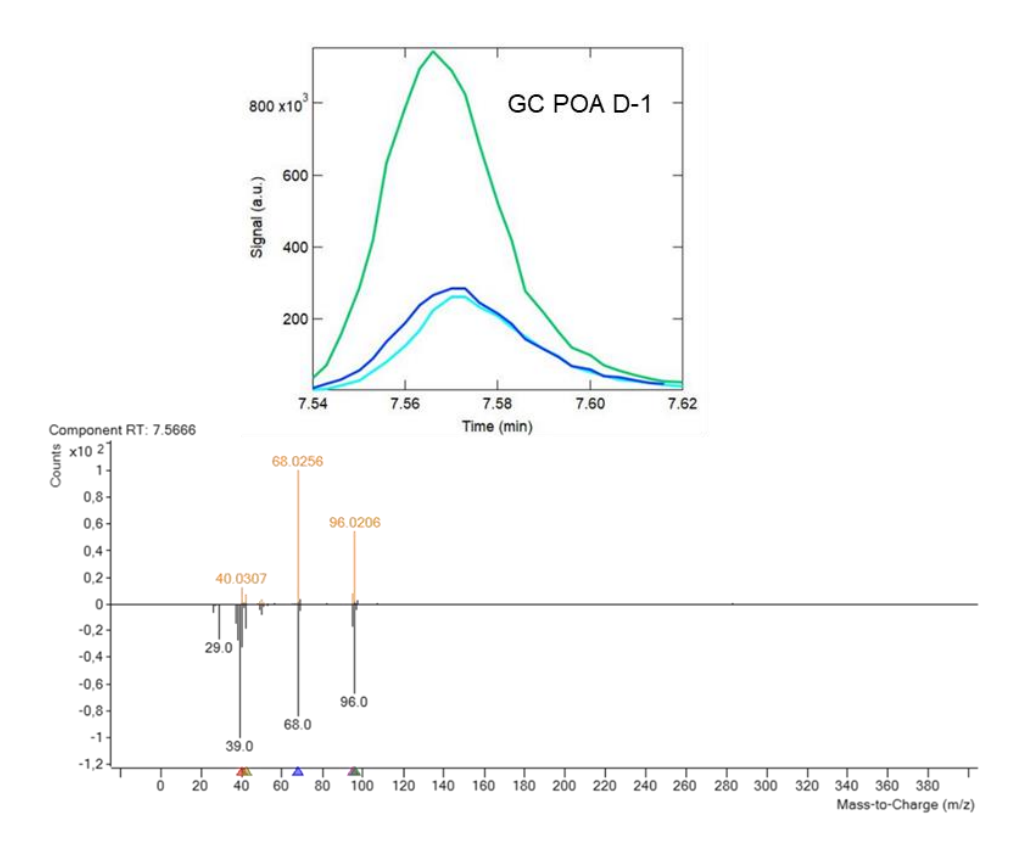


Figure S26. Chromatographic response of the feature base peak (m/z = 68.0256) and head-to-tail EI mass spectra of the POA diesel marker GC-POA D-1 and the 2H-pyran-2-one from GC-QToF data (acquisition started at 40 m/z).

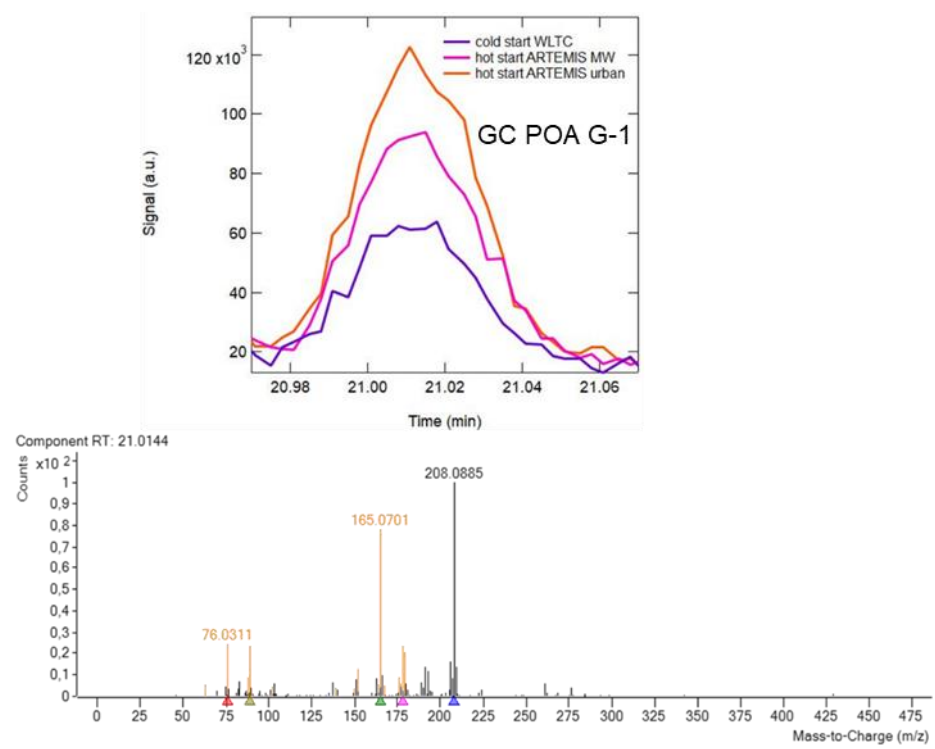


Figure S27. Chromatographic response of the feature base peak (m/z = 208.0885) and the EI mass spectra of the POA gasoline marker GC POA G-1 from GC-QToF data (acquisition started at 40 m/z).

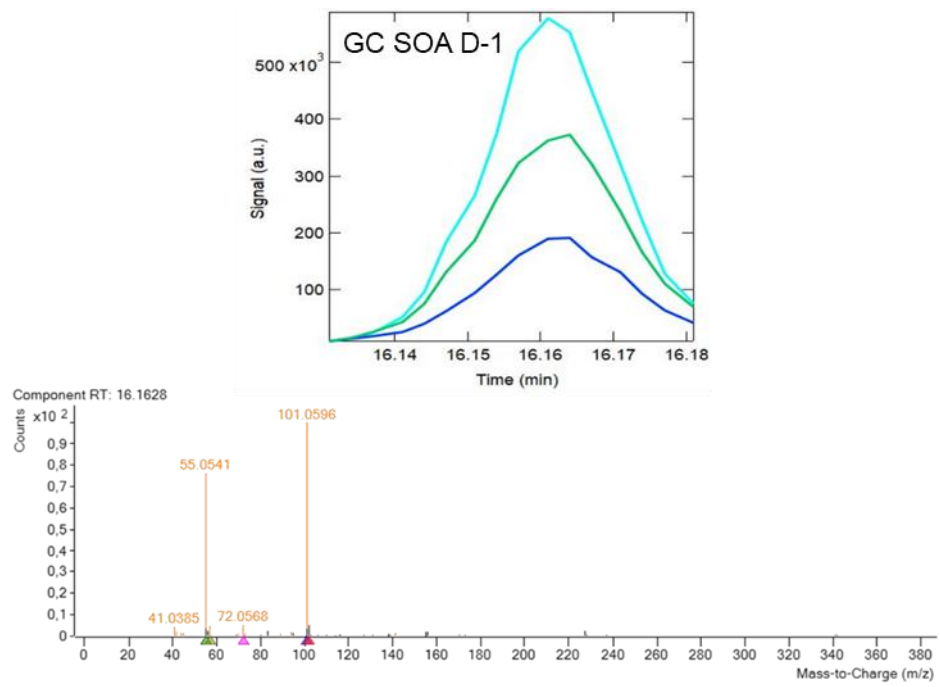


Figure S28. Chromatographic response of the feature base peak (m/z = 101.0597) and the EI mass spectra of the SOA diesel marker GC SOA D-1 from GC-QToF data (acquisition started at 40 m/z).

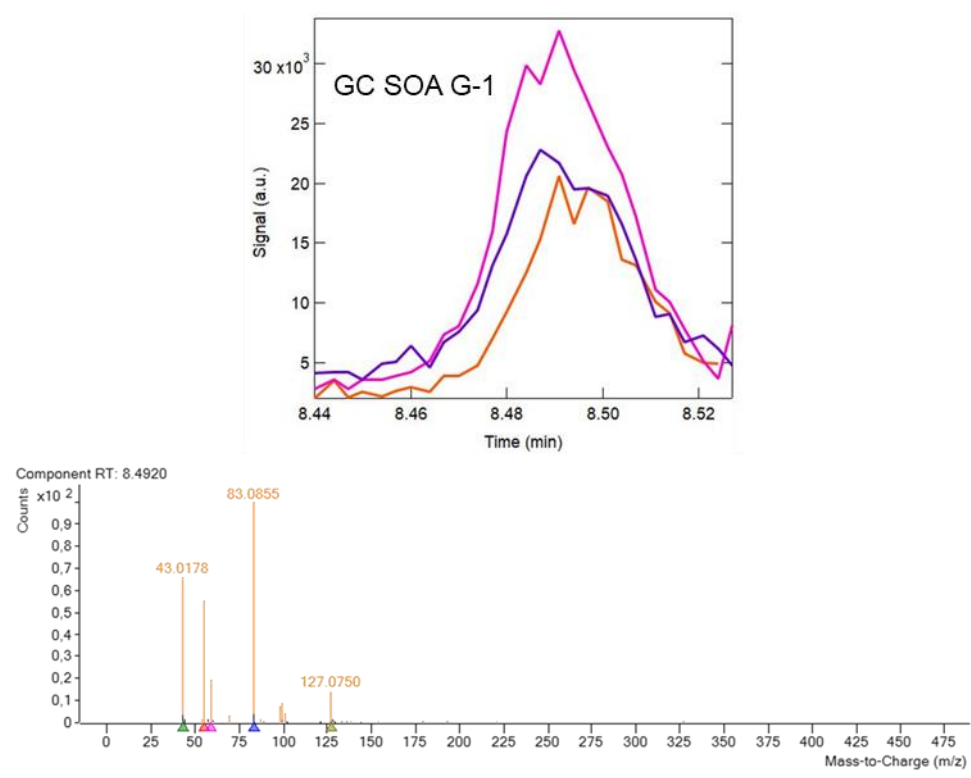


Figure S29. Chromatographic response of the feature base peak (m/z = 127.0750) and the EI mass spectra of for one SOA gasoline marker GC SOA G-1 from GC-QToF data (acquisition started at 40 m/z).

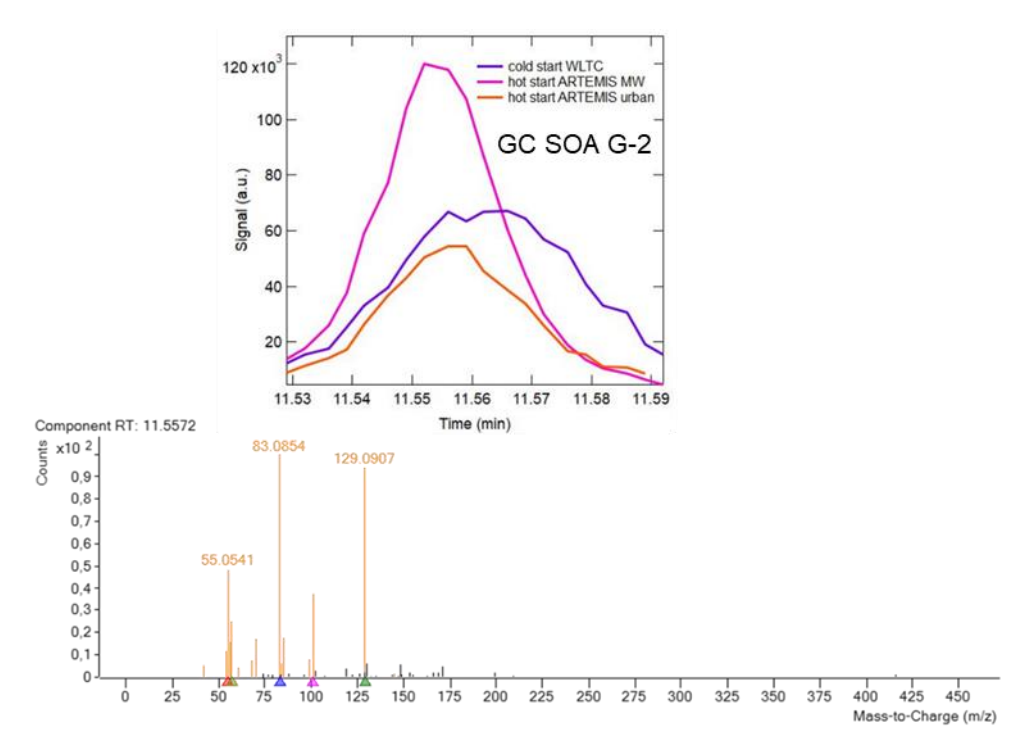


Figure S30. Chromatographic response of the feature base peak (m/z = 129.0909) and the EI mass spectra of one SOA gasoline marker GC SOA G-2 from GC-QToF data (acquisition started at 40 m/z).